

MASTERS THESIS

M-3937

DEININGER, Jr., James William  
PETROLOGY OF THE WRANGELL VOLCANICS NEAR  
NABESNA, ALASKA.

University of Alaska, M.S., 1972  
Geology

University Microfilms, A XEROX Company, Ann Arbor, Michigan

© 1973

JAMES WILLIAM DEININGER, Jr.

ALL RIGHTS RESERVED

PETROLOGY OF THE WRANGELL VOLCANICS  
NEAR NABESNA, ALASKA

A  
THESIS

Presented to the Faculty of the  
University of Alaska in Partial Fulfillment  
Of the Requirements  
for the Degree of  
MASTER OF SCIENCE

by

James W. Deininger, BA  
College, Alaska  
May, 1972

PETROLOGY OF THE WRANGELL VOLCANICS  
NEAR NABESNA, ALASKA

APPROVED:

W. B. Hawley

W. H. Sillit  
By Narayan Naidoo

Donald P. Turner

Robert B. Taylor

Chairman

Carl S. Benson

Department Head

APPROVED:

Carl H. Bechtel Date 12/13/71

Dean of the College of Earth  
Sciences and Mineral Industry

G. Rae

Vice President for Research and Advanced Study

PLEASE NOTE:

Some pages may have

indistinct print.

Filmed as received.

University Microfilms, A Xerox Education Company

## ABSTRACT

The Wrangell Mountains are underlain by a thick sequence of late Tertiary and Quaternary volcanics. In the Nabesna area, this sequence is represented by nearly 4000 feet of augite-hypersthene andesites, hypersthene or hornblende dacites, and tholeiitic basalts. The relative volumetric abundance of these rock types is as follows: pyroxene andesite, 59%; dacite, 26%; and tholeiitic basalt, 13%. The oldest flows in the Wait Creek Section were determined to be at least 13.5 ( $\pm 0.8$ ) m.y. old by  $K^{40}/Ar^{40}$  whole rock radiometric dating techniques.

The association, relative volume, orogenic setting, and mineralogy and chemical composition of the flow units indicate that the Wrangell volcanics belong to the calc-alkali rock series. The decline of FeO and MgO, and invariant Na<sub>2</sub>O and K<sub>2</sub>O with increasing SiO<sub>2</sub>, is generally considered to be characteristic of calc-alkali volcanics with continental affinities.

Diagrams showing sequential variation in element concentration, and multivariate discriminant relations reflect a complex history of the Wrangell volcanics. Changes in the element concentration of rock units in the sequence show compositional variation to be greater in the andesites and basalts, than in the dacites. Multivariate discriminant analysis distinguishes two compositional groups which correspond to rock type. The dacites form a group which is distinct from the andesites; basalts cannot be similarly separated from andesites. Standard silica, total alkalis, and FMA variation diagrams show sympathetic compositional fields within these two groups. However, these fields do not show any cross-group correlation.

In the light of andesite theory these data imply that the Wrangell volcanics were probably derived by the partial melting of the lower crust at various depths, to form batches of magma which show some variation due to fractional crystallization.

## ACKNOWLEDGMENTS

Special thanks are given to Dr. Dipak K. Ray formerly of the University of Alaska Geology Department and Geophysical Institute for his invaluable advise and theoretical and practical discussions prior to going in the field. Thanks are also in order for Dr. Daniel Hawkins of the Geology Department for exposing the writer to a sound theoretical grounding. Gratitude is acknowledged to Dr. Carl Benson, Geology Department Head for a grant from the Geology Department that largely covered field expenses. Thanks are also extended to Mr. Chuck Hawley for the loan of indispensable field equipment, and flyovers which monitored the writer's welfare in the field. Excellent air transportation was provided by Bill Ellis of Devil's Mountain Lodge.

Laboratory research was carried out under the direction of Dr. Robert Forbes of the Geology Department and Geophysical Institute, with additional technical advice of Drs. D. L. Turner and P. D. Rao of the Geology Department and Geophysical Institute and Mineral Engineering Department respectively. Dr. Forbes' critical reading and valuable comments on this manuscript is also greatly appreciated.

## TABLE OF CONTENTS

	Page
ABSTRACT	iii
ACKNOWLEDGMENT	v
TABLE OF CONTENTS	vi
LIST OF FIGURES	viii
LIST OF TABLES	ix
LIST OF PLATES	ix
CHAPTER I INTRODUCTION	1
Location of the Study Area	1
Plan of Investigation	1
Analytical Methods	
CHAPTER II GEOLOGIC SETTING	6
Regional Geology	6
CHAPTER III THEORIES ON THE ORIGIN OF ANDESITE	12
Introduction	12
Distribution and Classification of Andesites	12
Andesite Distribution in Time	14
Andesite Theory	14
CHAPTER IV STRATIGRAPHY OF THE WRANGELL VOLCANICS	19
Introduction	19
Contacts	21
Lithology	21
Attitude	26
Eruptive History	26
CHAPTER V PETROLOGY OF THE FLOWS	29
Petrography	29
Basalts	29
Andesites	31
Dacites	33
Plagioclase Composition of the Flow Units	34
Chemical Analyses of Rock Units	34
Stepwise Discriminant Analysis	46
Variation Diagrams	50
Paragenesis	52



	Page
CHAPTER VI    SUMMARY AND CONCLUSIONS	57
Conclusions	57
The Wrangell volcanics and the Andesite Problem	58
Recommendations for Further Work	60
REFERENCES CITED	62

## LIST OF FIGURES

	Page
FIGURE 1. Index map showing location of study area in relation to the major tectonic elements of Alaska.	2
FIGURE 2. Reconnaissance geologic map of the southeast corner of the Nabesna B-5 quadrangle, Alaska.	5
FIGURE 3. Diagrammatic stratigraphic section at Wait Creek showing lithology of individual flows.	22
FIGURE 4. Generalized sections depicted for Wait and Cabin Creeks including probable correlation of sedimentary interbeds.	25
FIGURE 5. Diagram showing the maximum, minimum, and average (dashed line) anorthite content of the plagioclase in the samples from Wait Creek.	37
FIGURE 6. Diagram showing the maximum, minimum, and average (dashed line) anorthite content of plagioclase in the samples from Cabin Creek.	38
FIGURE 7a. Diagram showing the $\text{Na}_2\text{O}$ and $\text{K}_2\text{O}$ variation in rock samples from the Wait Creek Section.	42
FIGURE 7b. Diagram showing the $\text{MgO}$ variation in rock samples from the Wait Creek Section.	43
FIGURE 7c. Diagram showing the variation in total iron content of rock samples from the Wait Creek Section	44
FIGURE 7d. Diagram showing the $\text{SiO}_2$ variation in rock samples from the Wait Creek Section.	45
FIGURE 8. Plot of the first and second canonical variables showing the separation of dacites (D) from andesites (A). The single basalt analyzed is represented by the * in the lower left hand corner of the graph, the * indicates group means.	49
FIGURE 9. Silica variation diagrams for analyzed rock samples from the Wait Creek Section.	51
FIGURE 10. Diagram showing the variation of total alkalis with increasing $\text{SiO}_2$ . Compositional fields taken from Kuno (1965).	53

	Page
<b>FIGURE 11.</b> FMA triangular diagram showing plots of analyzed rock samples from the Wait Creek Section. Differentiation trends taken from Yoder and Tilley, 1962, p. 424.	54

## LIST OF TABLES

<b>TABLE 1.</b> Table of the major formations occurring in the Wrangell Mountains and immediately surrounding areas compiled from Smith (1954) and MacKevett (1970).	7
<b>TABLE 2.</b> Field description of principle rock units in the Wait Creek Section. Table is keyed to lithologies in Figure 3.	23
<b>TABLE 3.</b> Estimated modes for rock specimens from the Wait Creek Section (in stratigraphic succession).	30
<b>TABLE 4.</b> Estimated modes for rock specimens from the Wait Creek Section (in stratigraphic succession).	32
<b>TABLE 5.</b> Anorthite content in rocks from the Wait Creek Section (in stratigraphic succession).	35
<b>TABLE 6.</b> Anorthite content in rocks from the Cabin Creek Section (in stratigraphic succession).	36
<b>TABLE 7.</b> Partial chemical analyses of rock samples from the Wait Creek Section.	40
<b>TABLE 8.</b> Discriminant Function Table.	47
<b>TABLE 9.</b> Summary Table.	48

## LIST OF PLATES

<b>PLATE 1.</b> Wait Creek Section: dc = hypersthene dacite; and = pyroxene andesite; ivc = lahar-mudflow sedimentary interbeds; tb = tholeiitic basalt; Qd = undifferentiated Quaternary deposits.	20
<b>PLATE 2.</b> Cabin Creek Section: and = pyroxene andesite; ivc = lahar-mudflow sedimentary interbeds; uMes = undifferentiated Mesozoic rocks.	20

## CHAPTER I

### INTRODUCTION

#### Location of the Study Area

The study area is located on the north slope of the Wrangell Mountains, in the Nabesna District, approximately 250 air miles east-northeast of Anchorage, Alaska. The Wrangell Mountains are overlain by a thick section of Tertiary and Quaternary volcanic rocks, forming a volcanic pile of approximately 7,000 square miles which contains several peaks rising over 12,000 feet above sea level. On a clear day four major volcanic peaks, Mount Drum, Mount Blackburn, Mount Sanford, and Mount Wrangell, can be seen from vantage points in the study area. The Wrangell volcanic pile lies in a tectonic trough between the Nutzotin Mountains, which form the eastern extension of the Alaska Range, and the Chugach Mountains, which form a segment of the Coast Range (see Figure 1).

#### Plan of Investigation

The plan of investigation included the collection of samples of the flow units composing the Wrangell Pile for petrographic and chemical analysis, with the hope of reconstructing the eruptive history and genesis of the extrusives.

Samples were collected from each identifiable flow or at 100 foot intervals if the individual flows were not discernable. Sections were measured and studied at several localities (see Figure 2). Reconnaissance geologic mapping was carried out in the intervening areas to establish stratigraphic correlation between sections.

Measurement of linear structural elements (i.e. vesicle elongation and vesicle trains) and inter-flow contacts was also attempted, but time did not permit the

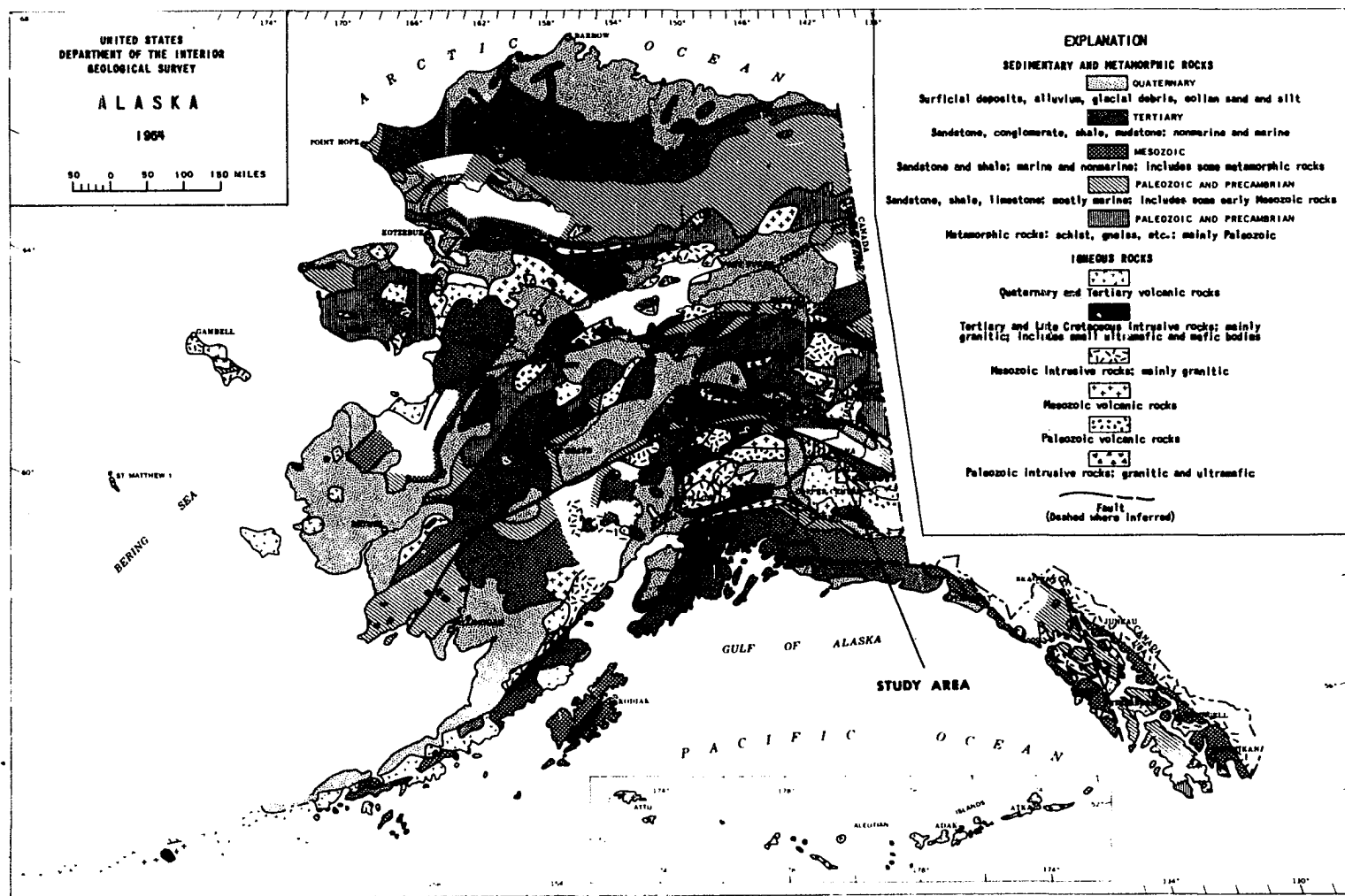


FIGURE 1. Index map showing location of study area in relation to the major tectonic elements in Alaska.

acquisition of sufficient data for a statistical study. Attitudes of inter-flow contacts were in general very low and variable over short distances.

Where possible, only fresh samples were collected, which contained a minimum number of vesicles and phenocrysts. Samples for  $K^{40}/Ar^{40}$  were also taken in the Cabin Creek Section, with particular attention to the lahar-mudflow interbeds that are marker horizons in several of the sections. Many of these samples however proved to be unsatisfactory for dating due to alteration and/or glass content of plagioclase phenocrysts and groundmass.

### Analytical Techniques

Thin sections of representative rock units were studied petrographically, which included identification of minerals present, estimated mode, and fabric description. The anorthite content of the plagioclase phenocrysts was determined with the universal stage, using the Rittman Zone method (Emmons, 1943); and the high temperature plagioclase composition curves of Troger (1956) for sections perpendicular to (010). Ten grains were measured, or as many as could be found if less than 10 were present in a thin section. Alkali feldspar content was determined by staining rock chips, using the sodium cobaltinitrite method.

Partial chemical analyses of whole rocks were accomplished by preparing lithium metaborate fusions as defined by Ingemells (1962). Sodium and potassium were determined on a Model K343 flame photometer, at the Geophysical Institute of the University of Alaska. Silicon, total iron (as FeO), and magnesium were determined on a Perkin-Elmer 303 atomic absorption spectrophotometer at the Mineral Engineering Department of the University of Alaska. Standards used in

flame photometric and atomic absorption analyses were prepared from U.S.G.S. standards G-2, DTS-1, and BCR-1, and the French standard BR-Basalt (Roubault et. al., 1968, p. 394).

## EXPLANATION

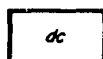
### ROCK UNITS

#### UNCONSOLIDATED QUATERNARY DEPOSITS

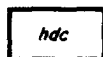


*Undifferentiated alluvium, landslide debris, and talus*

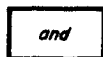
#### QUATERNARY AND TERTIARY ROCKS



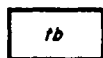
*Hypersthene dacites*



*Hornblende dacites*



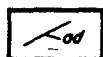
*Augite-hypersthene andesites*



*Tholeiitic basalts*



*Intercalated mudflow and laharic deposits,  
locally reworked by paleostreams*



*Andesitic dike*

#### MESOZIC ROCKS



*Undifferentiated massive and thin-bedded limestones,  
greenstone, and porphyritic intrusive rock  
(Contact after D.H. Richter, personal communication 1970.)*

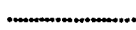
### MAP SYMBOLS



*Collected stratigraphic section*



*Contact, approximately located*



*Contact, covered*



*Dip and strike of flow units*



*Bearing and plunge of vesicle elongation*



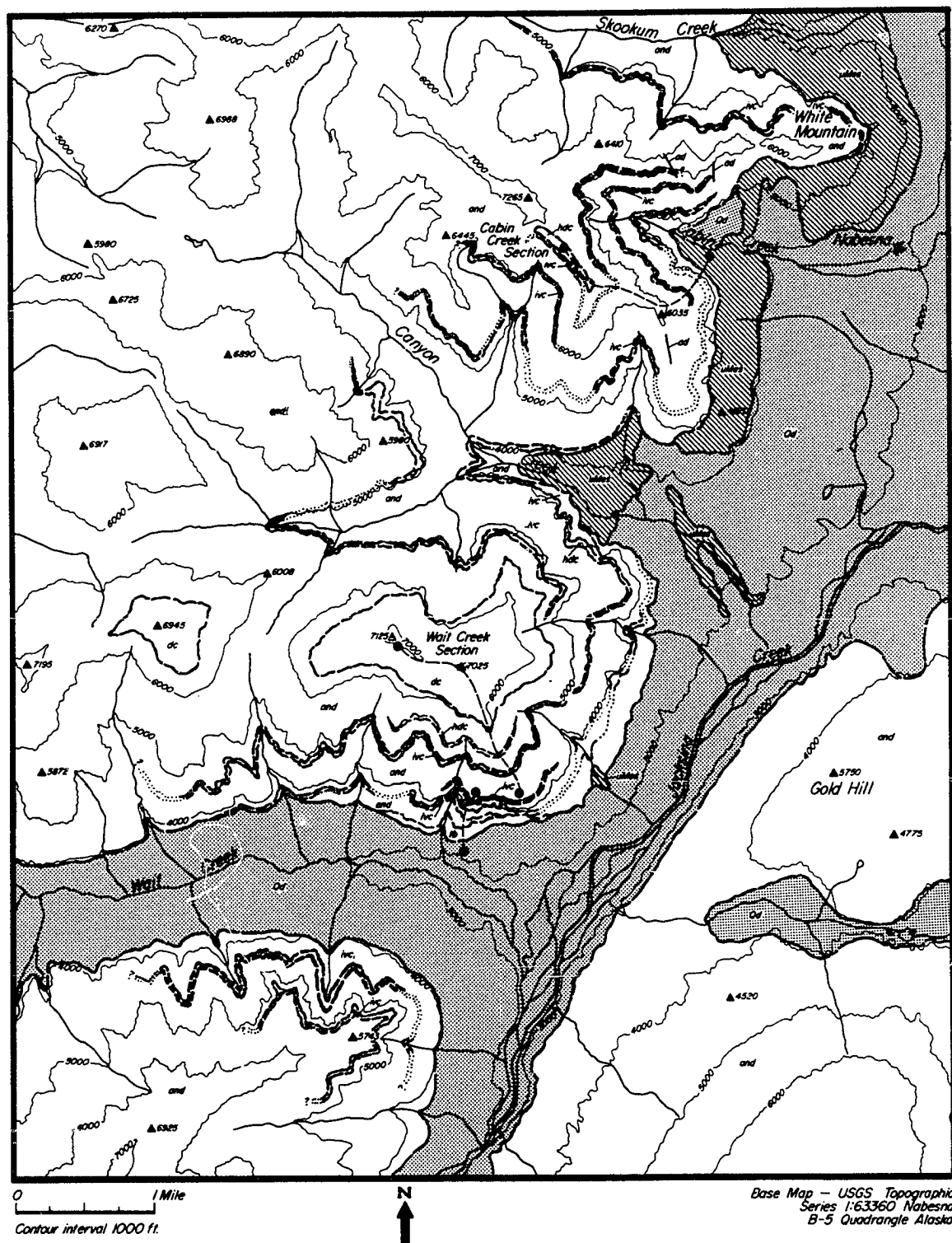


Figure 2 Reconnaissance Geologic Map, SE Corner Nabesna B-5 Quadrangle, Alaska.

## CHAPTER II

### GEOLOGIC SETTING

#### Regional Geology

The geologic history of the Wrangell Mountain area has been discussed by many writers from the turn of the century to the present. The first descriptions of any substance were those by Mendenhall and Schrader (1903) and Mendenhall (1905). Frequently reoccurring names in the geologic literature concerning this general area include Moffit, F. H., Capps, S. R., Wayland, R. G., and MacKevett, E. M. Moffit (1953) provides an extensive summary of his and others' earlier works on the north flank of the Wrangell Mountains. Wayland, in Moffit and Wayland (1943), wrote the first detailed report on the petrology and chemistry of the Wrangell lavas. Very recently MacKevett (1963) and (1970) has been carrying out an extensive, systematic geologic mapping program for the U.S. Geological Survey on the south slope of the Wrangell Range. Grantz's (1966) study of strike slip faults in Alaska discusses recent faulting immediately north of the study area. This faulting has been studied in greater detail by Richter (1971). The stratigraphy, geologic history, and structural relations that follow are principally from Capps (1916), Moffit and Wayland (1943), Moffit (1953), MacKevett (1970), Denton and Armstrong (1969), and Richter (1971). Table 1 summarizes the principle rock units which occur on the north and south flanks of the Wrangell Mountains.

The oldest known rocks in the Eastern Alaska Range are pelitic schists and gneiss with interbedded basic meta-igneous rocks. These poorly exposed, strongly metamorphosed rocks are difficult to decipher but are interpreted to be older than

TABLE 1. Table of the major formations occurring in the Wrangell Mountains and immediately surrounding areas compiled from Smith (1954) and MacKevett (1970).

<u>Geologic Age</u>	<u>Unit Name or Type Locality</u>	<u>General Description</u>
Miocene	QTW-volcanics	Flows with basal intercalated non-marine sediments. <sup>2</sup>
Eocene	Tw-pyroclastics	Agglomerate, flows, breccia, tuff, intercalated non-marine sediments. <sup>1</sup>
	Fredericka Fm.	Conglomerate, variegated clay, lenses of coal, non-marine. <sup>2</sup>
L. Cretaceous	McColl Ridge Fm	Coarse to fine grained sandstone, conglomerate, rare siltstone. <sup>2</sup>
	Chititu Fm.	Midstone, shale, sandstone, limestone, sandstone dikes. <sup>2</sup>
E.-L. Cretaceous	Moonshine Cr. Fm.	Fine grained siltstone, sandstone, and conglomerate. <sup>2</sup>
	Schultz Fm.	Thin bedded, resistant, silicious rocks. <sup>2</sup>
L. Cretaceous	Kotsina-Chitina District Kennicott Fm.	Black shale, sandstone, with small amounts of conglomerate and sandy shale. <sup>1</sup>
L. Jurassic	Kuskulana-Nizina District	Conglomerate, sandstone, limestone, shale. (Formerly Kennicott Fm.) <sup>1</sup>
M. Jurassic	Chitina District	Tuff. <sup>1</sup>
E. Jurassic	McCarthy Shale	Shale, black shale, argillite. <sup>1</sup>
L. Triassic	Nizina Limestone	Thinbedded limestone, some shale more abundant towards top. <sup>1</sup>
L. Triassic	Chitistone Ls.	Massive bedded limestone with thin shale partings. <sup>1</sup> Basaltic lava of greenstone habit. <sup>1</sup>
M.-L. Triassic	Nikolai Greenstone	Basal conglomerate and subaerial basaltic lava flows. <sup>2</sup> Lava, tuff, volcanic breccia interstratified with shale, limestone, sandstone, and conglomerate. <sup>1</sup>
Permian	Skolai Group	Weakly regionally metamorphosed sub-marine lavas and their derivatives overlain by marine sediments. <sup>2</sup>
Mississippian	Strelina Fm. and Klutina Group	Slate, schist, small amounts of limestone, tuff, and basalt flows. <sup>2</sup>

1. Smith (1954)

2. MacKevett (1970)

middle Devonian by Moffit and Wayland (1943). Structurally these rocks exhibit closely compressed folds whose axial planes are horizontal. The trend of the relatively more competent interbedded limestones is roughly parallel to the strike of the schistosity,  $S_2$ , though the original bedding,  $S_1$ , is not readily apparent. The folding and faulting that developed these extremely complex structures is believed by Moffit (1953, p. 176) to represent more than one period of deformation.

The Middle Devonian marks the submergence and consequent marine deposition of limestone, volcanic tuffs and basic lavas. Capps (1916) characterises this period as one of marine sedimentation with intermittent extrusion of lavas and pyroclastics with ever increasing frequency. The slates, schists, limestones, tuffs, and basaltic flows in the Eastern Alaska Range are scarce and not much more is known about them.

The Permian is noted for its large proportion of limestone, basic lava flows, and limey tuffs. These marine beds unconformably overlie older beds in the area indicating the end of an erosion period. Moffit and Wayland (1943) postulate two extended periods of marine deposition within this period of prolonged volcanic activity. They also note that although some of the volcanics show pillow structures, which are taken to indicate a marine environment, most flows are the result of subaerial extrusion. These Permian lavas are basaltic in character, commonly finely porphyritic and sometimes vesicular.

Paleozoic intrusives are in general not easily identified because of their degree of alteration and metamorphism. Mendenhall (1905) describes the intrusives of this age as being bodies of diorite and quartz diorite. The structure of these Late Paleozoic rocks is the result of a separate orogenic episode from that

of the Early Paleozoics as the folding and faulting is relatively less intense, and these Early Paleozoics are separated by an angular unconformity from the Late Paleozoics.

The Mesozoic cycle began with the deposition of eugeosynclinal deposits in the basins bordering small, actively denuding land-masses. The rock record consists of limestone, shale, arkose, conglomerate, as well as basaltic and andesitic lavas intruded by dikes, sills, and irregular bodies of granodiorite. The present structure of these rocks varies with the degree of competence of the beds. The less competent rocks are characterized by parallel folds with slightly overturned axial planes. A period of folding, uplift, and erosion preceded the Late Triassic deposition of limestones and shale. The Middle Jurassic marked the beginning of intermittent orogeny and uplift that formed the arcuate structural trends of the Wrangell, St. Elias, and Chugach Mountains. Intrusion and extensive mineralization occurred during the Middle to Late Mesozoic (Moffit, 1953, p. 182). These deep seated granitic rocks formed the roots of the Alaska Range as well as the hypabissal sills and dikes of the Nutzotin Mountains. Cretaceous time was marked by non-marine and estuarine deposition on the positive areas and graywacke sedimentation in the marginal troughs. Marine deposition ceased at the end of Cretaceous time in the Wrangell, St. Elias, and Chugach Mountain region but continued on a much smaller scale in localized basins to the north and south of this belt.

Early Cenozoic deposits are missing from the record and Middle Eocene gravels, coal measures, and lavas unconformably overlie Late Mesozoic rocks. These Late Cretaceous and Early Tertiary formations are only mildly warped and

locally faulted. Gravels and coal beds are not abundant in the Nabesna area where lavas of basic to intermediate composition comprise most of the Cenozoic section. The first Wrangell lava flows were extruded upon a well developed sub-aerial erosion surface. These lavas formed a thick layered sequence before the beginning of Pleistocene glaciation. Eruption of lavas continued on a decreasing scale through the Pleistocene and Holocene, almost up to the beginning of historic time. Intrusive activity in Cenozoic time was restricted to dikes and sills of basaltic and dacitic compositions.

The Pleistocene in the Eastern Alaska Range was one of a sequence of advance, coalescence, and retreat of alpine glaciers. Even today the Wrangell Mountains retain extensive glacial systems. The lower peaks have been extensively eroded by ice, and the U-shaped stream valleys are filled with glacial debris and outwash. Capps (1940, p. 155) cites evidence for at least two periods of glacial maxima and correlates these with the Illinoian and Wisconsin advances (*ibid.*, p. 74). In Alaska these are equivalent to the Eklutna and Naptown glaciations, respectively (Pewe and Hopkins, 1965). Evidence for earlier advances is not readily delineated as the earlier glacial deposits have been destroyed and incorporated in later advances. During the advance in Naptown time, glacier ice occupied the entire Copper River drainage basin. No attempts have been made to delimit the extent of Neoglaciation but it can be assumed that it occurred in this area as it did in other parts of Alaska. Today, the general trend seems to be one of slow and fluctuating recession of alpine glaciers.

Active Quaternary faulting has additionally complicated the regional structure. Grantz (1966) has noted and described the Denali fault to be largely a high

angle, right-lateral strike slip fault. Richter (1971) has done detailed field work and air photo interpretation on these two fault systems, which form strong linear trends immediately north of the Nabesna-Slana area. The older, Early Pliocene Denali fault system is proposed by Richter to be over 2000 km. in length with a minimum strike slip of 200 km. The rate of slip, deduced by offset of Pleistocene and Holocene geomorphic features, ranges from 1.1 to 3.5 cm/yr. The younger Totschunda fault system, age 650,000 yrs., is at least 150 km. in length showing a 9 to 10 km. strike slip component and a vertical slip component of 1500 m., the southwest block being relatively upthrown. The rate of movement along this persistently active fault has been determined to vary between 0.9 to 3.3 cm/yr. The magnitude of these proportions alone indicate that these fault systems are by no means local features but are of regional tectonic importance. In addition Richter has correlated them with the Shakhwak fault of Western Canada and the Fairweather fault system of Southeastern Alaska, respectively.

Recent activity of the Wrangell volcanoes is not well documented. Mount Wrangell is the only remaining vent showing signs of volcanic activity. This activity consists of a steaming crater and many fumeroles around the rim of the ice filled caldera (Forbes, personal communication, 1971). A summary of the recent activity may be found in Furst (unpublished University of Alaska MS thesis, 1968, p. 8-9).

## CHAPTER III

### THEORIES ON THE ORIGIN OF ANDESITE

#### Introduction

During the July 1968 meeting of the International Upper Mantle Committee's Andesite Conference held in Eugene and Bend Oregon, Hisashi Kuno presented a paper entitled, "Andesite in Time and Space". In this paper, Kuno (1969, p.13), briefly summarized the importance and scope of andesites as follows:

"Andesite as defined by the  $\text{SiO}_2$ -alkali relation, occurs in various ages from early Precambrian (older than 2400 my.) to Recent. Although it is the most predominate rock type in the orogenic belts, it occurs also in the non-orogenic, continental areas, island arcs in oceans, and typical oceanic islands."

Perhaps the most perplexing problem in studying andesitic volcanism lies in the definition of andesite. The working definition given by Williams, Turner, and Gilbert (1956) was that of a fine-grained, porphyritic rock of intermediate composition. If one attempts to define andesites more precisely, in genetic terms, many problems ensue. Some of these problems may be better defined by looking at the regional distribution of andesites.

#### Distribution and Classification of Andesites

Andesitic lavas dominate the volcanism of the Pacific rim. This association led Marshall in 1911 to propose the well known 'Andesite Line'. Chayes (1964) recognized that Cenozoic andesitic volcanism occurs in four distinct geographic settings. The majority of chemical analyses he examined fell into a single geographic area; the discontinuous trenches along the rims of the oceans. The remaining three areas are; the islands of the open ocean, Mediterranean or



shallow sea areas, and the stable continent. Daly (see Tilley, 1950) distinguishes two tectonic settings in which andesites are found, and has calculated the relative abundances of rock types in these settings. Along the Pacific rim the relative abundance by volume of rock type is as follows:

Basalt . . . . .	32%
Andesite . . . . .	45
oceanic and stable area type . . .	4
calc-alkaline type . . . . .	41
Rhyolite . . . . .	22
Rest . . . . .	1
	<u>100%</u>

This striking abundance of andesite over other rock types is known as the volume problem and must be considered in any theory of andesite origin involving fractionation from a parent melt (see Kuno, 1969).

These attempts to correlate worldwide andesitic volcanism with tectonic setting emphasize that the chemical composition of andesitic rocks is not normally distributed about a single average, but tends to have a bimodal distribution. Tilley (1950) recognized two types of andesites, a tholeiitic andesite and a 'true', or orogenic andesite. The chemical basis for this distinction lies in fractionation trends defined by variation in the FeO/MgO ratio. Kuno (1969) subdivided the andesites of Japan, Manchuria, and Korea on the basis of compositional fields on an alkali vs. silica diagram. The andesites with high total alkalis were called alkali andesites, and the low alkali andesites were classified as calc-alkali andesites. In addition he found a transitional zone between the alkali and calc-alkali andesites which he defined as high alumina andesite. Other methods of distinguishing andesite are based upon the normative and modal occurrences of characteristic minerals. Normative quartz and color index is considered by Chayes

(1969) to be distinctive, in contrast to other porphyritic eruptives of intermediate composition. Rosenbush (1923) proposed that andesites be those intermediate, porphyritic extrusives with a normative anorthite content more sodic than calcic oligoclase, and less calcic than sodic labradorite.

### Andesite Distribution in Time

To this point the discussion has centered about Cenozoic andesites as these extrusives are by far the most abundant in that Era, but they are by no means restricted to that Era. Precambrian andesites have been reported from the Canadian Shield by Baragar and Goodwin (1969). Kuno (1969) reports Paleozoic and Mesozoic andesites in the stratigraphic sections of Japan, Korea, and Manchuria. The relative abundance of andesites falls off sharply in the geologic column with increasing age. The skewing of this distribution in time may reflect the cumulative effect of alteration and erosion with time. In addition, andesite flows comprise deposits of relatively small extent in the highly energetic areas of tectonic activity; conditions which are not conducive to preservation. These older andesites are difficult to apply to the problem because of the difficulties involved in reconstructing their original tectonic setting.

### Andesite Theory

The interrelationship of basalts and orogenic andesites has had a strong influence on the theories proposed for the origin of andesite. Daly (Tilley, 1950) calculated that, without regard to tectonic setting, basalts are five times more abundant than all the other effusives in the world. Tilley (1950) advocated fractionation of a primary basalt magma with subordinate silicic assimilation to produce

andesite. He also proposed two fractionation trends, an iron enrichment or tholeiitic trend, and an iron depletion or orogenic andesite trend.

The concept of magma type originated with Bailey et. al. (1924) who recognized two magma types, plateau basalts and nonporphyritic central basalts in the Mull suite. Tomata (1932) proposed that since olivine basalts are ubiquitous to oceanic and continental settings with tholeiites restricted to continents, that olivine basalt was the parental magma. Tholeiite must then be derived by assimilation of sialic material. Kennedy (1933) recognized that these two magma types occurred on a world-wide scale. MacDonald (1944) recognized the reaction relationship of Bowen in the Hawaiian volcanic suite. MacDonald experimentally reheated a picrite basalt containing enstatite-augite which on recrystallization formed hypersthene and augite with the loss of olivine. He further recognized the presence of tholeiites as basal flows on the Hawaiian Islands. As a consequence he proposed that tholeiite was the parental magma, not olivine basalt. Recognizing this reaction relation and fractionation trend of iron enrichment to produce the 'andesites' typical of the tholeiitic provinces, Tilley proposed an iron depletion trend including sialic contamination to produce orogenic andesites.

Kuno's extensive work (1950), (1953), (1959) in Japan, Korea, and Manchuria also led him to support fractional crystallization of a tholeiitic parent to produce andesites. His pigeonitic trend reflects alkali enrichment whereas his hypersthene trend reflects alkali depletion and contamination by assimilation of crustal material. These derivatives from the hypersthene trend are the calc-alkali rock suite (Kuno, 1969).

In his study of the calc-alkali lavas of the Paricutin Volcano, Mexico, Wilcox (1954) favored the process of assimilation of granitic basement with fractionation of a basaltic parent to produce the observed andesites. He presents thermodynamic calculations to prove the feasibility of remelting and assimilation as physically demonstrated by incorporated xenoliths in the andesitic pyroclastics.

Experimental support for fractionation of a tholeiitic basalt parent to produce two andesite types comes from Osborn (1959). In the oxide system  $\text{MgO}-\text{FeO}-\text{Fe}_2\text{O}_3-\text{SiO}_2$  when bulk chemical composition remains constant, partial pressure of oxygen decreases and the alkali or non-orogenic derivatives result. Where partial pressure of oxygen increases, total composition does not remain constant and the calc-alkali (orogenic) derivatives result. Control of partial pressure of oxygen is proportional to the water pressure of the system which is probably high due to the presence of water rich sediments in the trenches of orogenic belts.

Green and Ringwood's (1966), (1969) experimental high pressure studies on synthetic and natural rocks led them to conclude a two-step partial melting process for andesite generation. The first stage of the process involves partial melting of quartz eclogite at 80-100 km. depth to produce basalt. The second stage involves further partial melting or fractionation of this hydrous basalt or amphibolite at 15-80 km. depth to produce andesite.

From trace element studies Taylor and White (1966) and Taylor (1969) propose a two stage derivation of andesites from primitive upper mantle material. Separation of the low melting fraction from the mantle peridotite produces pyrolite which again undergoes partial melting in orogenic areas to produce an andesite magma.

Gorshkov (1969) notes that where orogenic andesites occur, they are by far the most abundant rock type or the only rock type in some cases. In this regard he concludes that there must be a primary andesite magma to produce such vast quantities of chemically and mineralogically similar material.

Dickinson (1968) from his review of island arc volcanism, suggested fractional crystallization or partial melting of the mantle at varying pressures to produce andesites. He proposed that the variation of  $K_2O$  with  $SiO_2$  reflects the distribution of potassium between the solid and liquid phases at varying pressures down the subducting plate.

Waters (1961) takes exception to the previous theories involving a single parental basalt magma. He notes that the striking pattern of crystallization differentiation reflects a convergence toward a granite rather than backward toward a basalt. Hence he suggests a parental basalt for each fractionation trend proposed.

Recent developments in tectonic theory involving ocean floor spreading include speculation on the mechanism that produced the observed distribution of extrusives in orogenic belts. The spreading outward by the ocean floor from the mid-oceanic ridges was revived by Oliver and Sykes (1966). Where the oceanic plate dives beneath the continental plate it is marked by a planar zone of earthquake foci (Benioff, 1954) now called the benioff zone. According to Raleigh and Lee (1969) the subducting oceanic crust with its sediments is conveyed down the benioff zone to a level where melting occurs either by rebound of depressed isotherms or shock release pressure fronts. Green and Ringwood (1969) have shown experimentally that partial melting of a basalt in the presence of water at around 10 kb. pressure could give rise to the calc-alkali series. The subducting plate

provides an almost inexhaustible source of material for either partial melting or contamination of a basalt parent to produce the calc-alkaline volcanism on the continental side of these subducting plates.

## CHAPTER IV

### STRATIGRAPHY OF THE WRANGELL VOLCANICS

#### Introduction

The Wrangell volcanics comprise a sequence of flows nearly 4000 feet thick in the Nabesna area. In some localities, these flows unconformably overlie Tertiary pyroclastics. Where the pyroclastics are not present the Wrangell flow units unconformably overlie Triassic rocks, which are amygdaloidal basalts and massive, recrystallized limestones. In a few localities the base of the section is covered by Quaternary and Holocene fluvial and colluvial deposits. The subaerial surface upon which these flows were extruded was one of moderate relief. The highest units in the Wrangell volcanic sequence crop out on the highest peaks in the area.

In the White River District, immediately to the east-southeast the oldest Wrangell flows were dated as Eocene on the basis of plant fossils (Moffit, 1953, p. 167). Moffit however, expressed some reservations as to the reliability of this age determination. In the Nabesna area, one of the oldest flows exposed in the Wait Creek Section was determined to be at least 13.5 ( $\pm 0.8$ ) m.y.\*, based upon a whole rock  $K^{40}/Ar^{40}$  date (personal communication, Dr. David Stone, University of Alaska, Geophysical Institute). This date appears to be fairly reliable, at least for a minimum age, as this rock has only a minor amount of glass in the groundmass.

Terrain developed on Wrangell volcanics is characteristically quite steep and rugged with considerable outcrop exposure. Generally flow units are massive in their basal and intermediate zones, with flow tops composed of highly fractured and/or scoriaceous crust. Within a single flow, vesicularity and the volumetric  $K^{40}/Ar^{40}$  determinations by Geochron Laboratories.



PLATE 1. Wait Creek Section: dc = hypersthene dacite; and = pyroxene andesite; ivc = lahar-mudflow sedimentary interbeds; tb = tholeiitic basalt; Qd = undifferentiated Quaternary deposits.



PLATE 2. Cabin Creek Section: and = pyroxene andesite; ivc = lahar-mudflow sedimentary interbeds; uMes = undifferentiated Mesozoic rocks.



percent of plagioclase phenocrysts appeared to vary randomly. There was a distinct, though slight tendency toward mafic mineral concentration in the basal zone of individual flow units.

### Contacts

Contacts between individual flow units are not always distinct, and in many cases they are concealed by grass or talus. The lateral continuity of individual flows is limited, as they cannot be traced over a half mile in outcrop. Interflow contacts are not always horizontal as flow units have locally filled topographic depressions, and some units are intertongued with other flows. Conclusive evidence for weathering or soil formation was not observed between flows except along the interface of the flows and intercalated deposits. Chilled, glassy lower contacts were conspicuously rare between flows.

### Lithology

Complete sections of the Wrangell volcanics include basal calc-alkali basalts, succeeded by augite andesites and augite-hypersthene andesites, with hornblende or hypersthene dacites at the top of the section. The most complete and best exposed section is located near Wait Creek (Figure 3), where individual basalt flows are on the order of 100 feet thick near the base of the stratigraphic section.

The intermediate zone in the Wait Creek section, about 2000 feet thick, is composed of basaltic andesites and augite-hypersthene andesites. Towards the top of this portion of the section, the andesite flows contain two flows of hornblende dacite composition. A particularly thick succession of andesitic flows immediately above the topmost lahar-mudflow deposit in the Wait Creek section (see Figure 3)

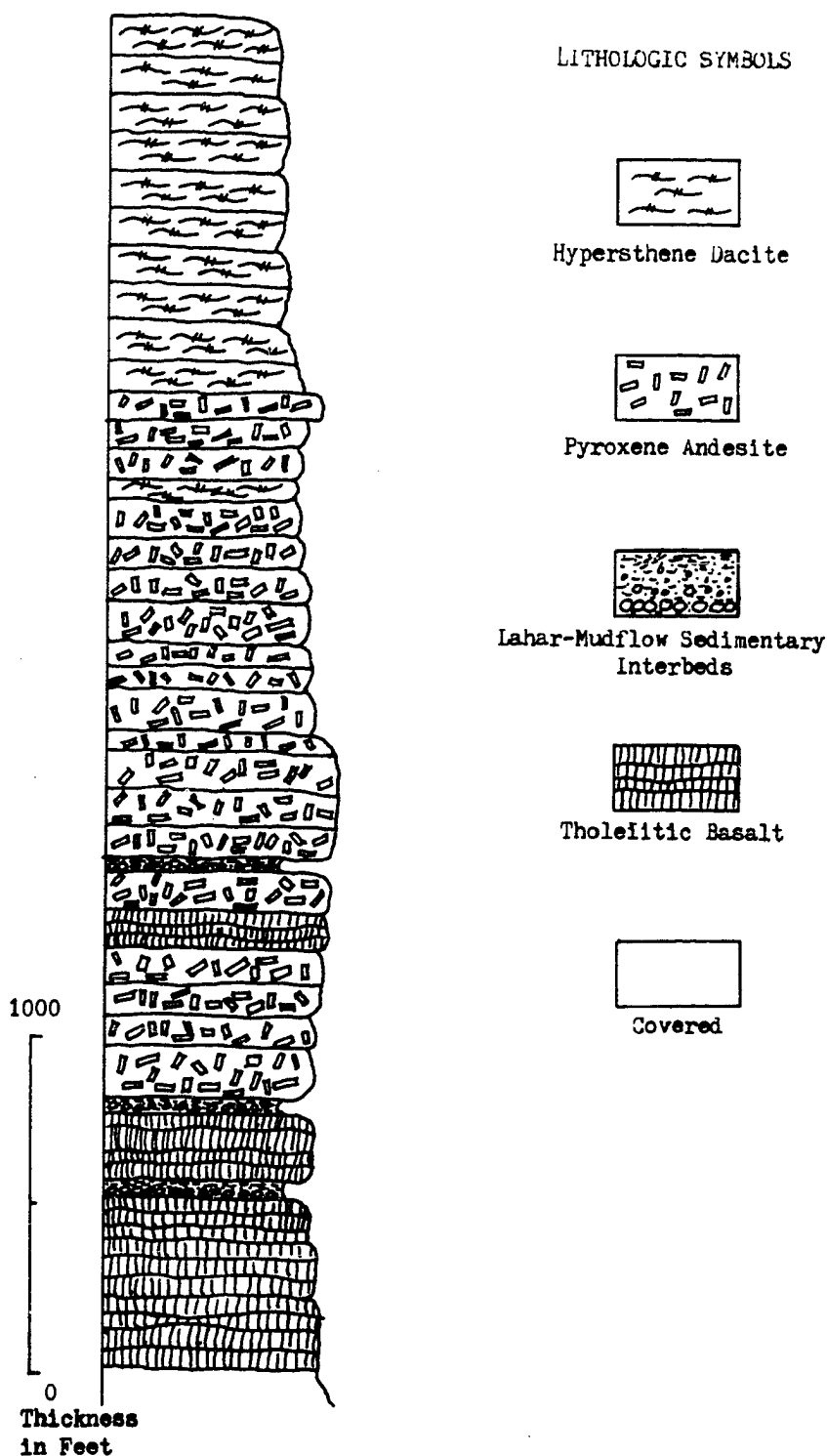


FIGURE 3. Diagrammatic stratigraphic section at Wait Creek showing lithology of individual flows.

**TABLE 2.** Field description of principle rock units in the Wait Creek Section. Table is keyed to lithologies in Figure 3.

### **HYPERSTHENE DACITES**

Light gray color; plagioclase phenocrysts in fine-grained groundmass; flows characterized by shaly parting; weathers to dark gray color; forms talus slopes consisting of large slabs; mainly rubble crops.

### **AUGITE-HYPERSTHENE ANDESITES**

Medium gray color; plagioclase and pyroxene phenocrysts in fine-grained groundmass; sometimes vesicular; irregularly fractured; weathers to a dark gray; forms blocky, resistant knobs in the talus, and sometimes near vertical cliff faces.

### **BASALTIC ANDESITES**

Dark gray color; plagioclase and pyroxene phenocrysts in a glassy groundmass; sometimes vesicular; weathers to a dark gray color; forms bold, resistant knobs and near vertical cliffs surrounded by talus.

### **LAHAR-MUDFLOW SEDIMENTARY INTERBEDS**

Conglomerates, sandstones and siltstones; grain size ranges from boulder to silt; unsorted conglomerates, poorly sorted sandstones and siltstones; clasts composed of andesitic and rhyolitic rock fragments, moderately indurated; unstratified except locally where upper sediments are crossbedded; weathers to light tan or dark brown depending on the lithology of clasts; not highly resistant to weathering, but boulder conglomerates may form steep cliff faces.

### **THOLEIITIC BASALTS**

Dark gray to almost black in color; fine-grained, dense rocks; sometimes vesicular, with vesicles filled by secondary calcite and/or epidote.

contains highly scoriaceous flow tops which are strongly iron stained and locally contain irregular masses of obsidian. These bright red iron stained bands attracted the attention of the early mapping geologists who in turn used it as an identifying character of the Wrangell lavas.

The top 1100 feet of the Wait Creek section is composed of hypersthene dacites. This interval is mostly mantled by dark, gray colored talus composed of massive slabs of lichen covered dacite. Hornblende dacites do not occur in this part of the Wait Creek section but they are present farther to the north in the Cabin Creek section.

The transition from mafic to more leucocratic and silicious volcanics, up section, is rather gradual. The andesitic part of the section contains two dacite flow units toward the top before the dacites become dominant in the section. Similarly, the basal horizon of the andesites is not sharply defined, and a few basalt flows are interbedded with the andesites immediately above the basal basalts.

Two types of dike rocks cut the Wrangell volcanics. Propylitized hornblende dacites occur near the top of the pyroxene andesite flows and extend into the hornblende dacite flows. The vesicular, anastomosing basaltic and andesitic dikes appear to be restricted to the lower part of the andesitic horizon of the section.

The three sedimentary interbeds occurring in the lower half of the Wait Creek section also occur in the Cabin Creek section (see Figure 4). Lithologically these units consist of unsorted, monolithologic boulder and pebble conglomerates, and are lacking in stratification. Moderately sorted, bedded and crossbedded sandstones and silstones also occur in these units but in subordinate amounts.

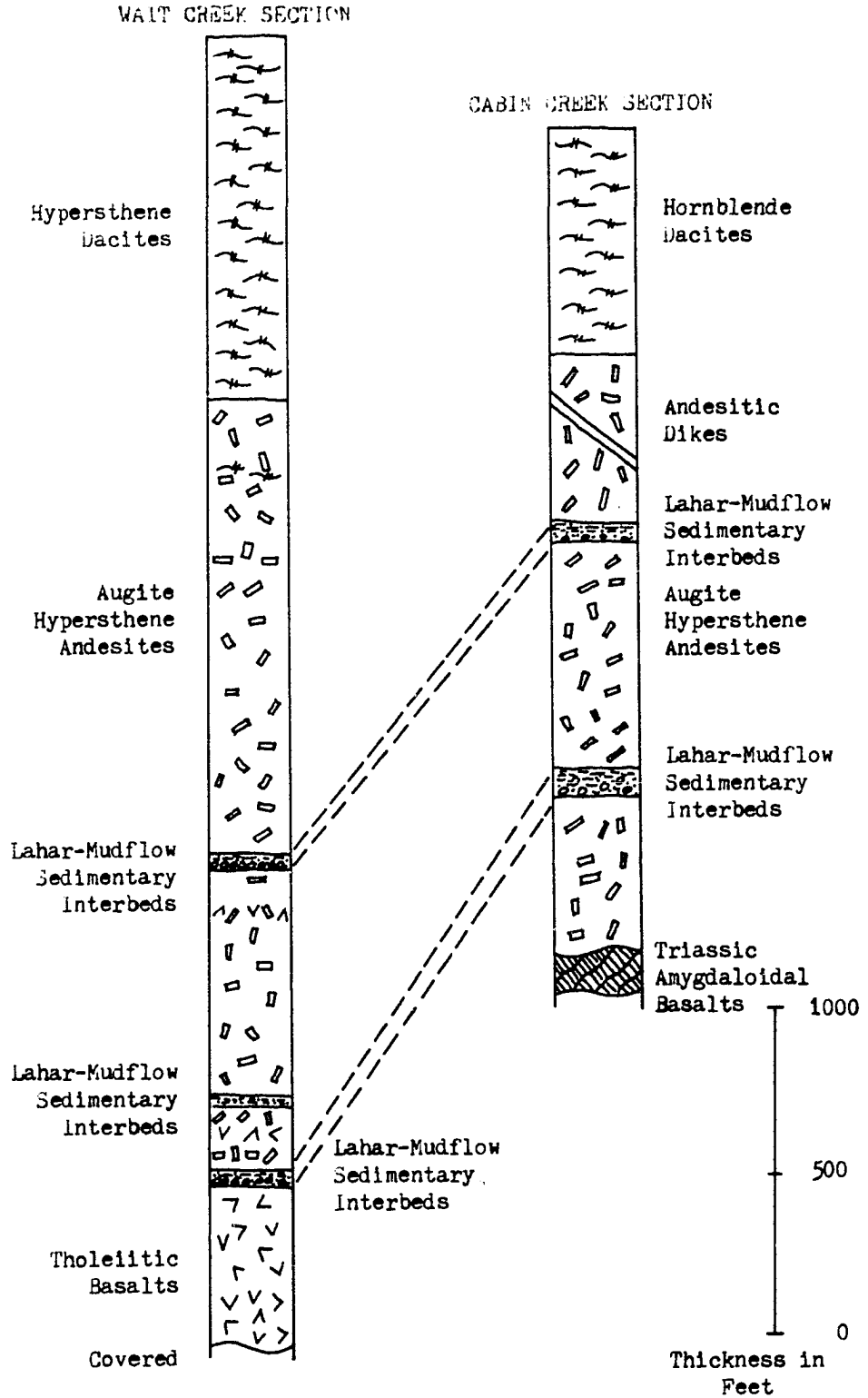


FIGURE 4. Generalized sections depicted for Wait and Cabin Creeks including probable correlation of sedimentary interbeds.

Two of these units appear to be continuous over an area of about 10 square miles though they pinch and swell irregularly. The third interbed is much thinner than the others and does not appear to be laterally extensive. Also its location in the stratigraphic succession varies throughout the study area indicating that probably it is not the same unit in different locations.

These intercalated deposits most likely originated as lahars and mudflows. Their unsorted character, general lack of bedding or stratification, rounding and plaining of the larger clasts, and the volcanic monolithology of the clasts support both these modes of origin. It is not likely that they are airfall deposits as one would expect to see some sort of stratification and the clasts would be more scoriaceous and angular shaped. Neither do they seem to be of glacial origin as one would expect diverse rock types, as can be seen in the thin veneer of glacial debris mantling the lower bedrock ridges in the local area.

### Attitude

The attitude of the Wrangell flow units is nearly horizontal and measurements taken on contacts between the sedimentary interbeds and andesitic flows indicate a gentle dip of  $3^{\circ}$  to  $6^{\circ}$  to the southwest. The Wrangell volcanics overlie with angular unconformity limestones and amygdaloidal basalts of Mesozoic age. The attitude of the limestone beds in the vicinity of White Mountain dips about  $35^{\circ}$  in a west-southwest direction.

### Eruptive History

The volcanoes of the Wrangell Mountains have never been conclusively documented as having erupted in historic time. Indian tales report eruptions (Moffit,

1943), but the reliability and chronology of these reports is suspect. Mt.

Wrangell is considered to be active, as it contains a number of actively degassing fumeroles around the rim of its ice filled caldera (Bingham, 1967, unpublished MS thesis, University of Alaska), and ash laden clouds have been erupted from its crater in historic time.

Based upon the relative degree of dissection of the prominent composite cones that comprise the backbone of the Wrangell Range, Mendenhall (1905, p. 57) dates the volcanoes in the following order beginning with the oldest; Mount Drum, Mount Blackburn, Mount Sanford, and Mount Wrangell.

The earliest flows in the eastern part of the Range have been dated to be of Eocene age (55-38 m.y.). In the Nabesna district, the earliest flows have a minimum age of 13.5 ( $\pm$  0.8) m.y. This great disparity may not be real as the oldest is based somewhat questionably on non-marine plant fossils, the other is based upon a minimum age, whole rock  $K^{40}/Ar^{40}$  date.

The primary mode of eruption of lavas was of the central vent type forming large, fairly steep-sided composite cones. Locally, the occurrence of abundant, anastomosing dikes, of similar mineralogy to that of the flows, suggests that fissure eruption may have contributed to the total thickness of the Wrangell volcanic succession. In addition to the prominent vents such as Mount Wrangell, smaller vents probably existed locally as a source of the flows in the Nabesna District. A small but thick wedge shaped deposit of pyroclastics occurs immediately to the north of the mapped area, the center of which is an endogenous rhyolitic dome. There is at least one other, but slightly smaller endogenous dacite dome, about a mile from the rhyolitic dome. It is possible that other domes are located in the

Nabesna District. These domes probably represent the sources for the volcanics observed in the Nabesna area. In addition the relative thickness compared to the lateral extent, about a half mile, of an individual flow and viscosity of andesitic melt suggests that the source is not too far distant. This multiplicity of local sources raises a problem in that the flows sampled in a single section may not have been erupted from the same source.



## CHAPTER V

### PETROLOGY

#### Petrography

##### Basalts

The olivine tholeiites and tholeiitic basalts possess a fine-grained granular texture but some transitional varieties may be slightly microporphyritic with an intersertal to intergranular groundmass. Visually estimated modes are tabulated in Table 3 only as basalts are not present in the Cabin Creek Section. Sodic labradorite comprises nearly three-fourths of these rocks by volume. It is the dominant phenocrystal phase in the microporphyritic varieties, and occurs as subhedral, lath shaped grains in the equigranular varieties. The remaining mode consists of euhedral, forsteritic olivine, anhedral to subhedral augite, and subhedral hypersthene. Augite is two to three times as abundant as hypersthene, and both taken together nearly equal the olivine in abundance where olivine is present. Minor amounts of brown volcanic glass and euhedral opaques, mostly magnetite, are also present in the groundmass. Vesicles where present commonly contain the secondary minerals calcite and epidote.

Plagioclase grains exhibit carlsbad-albite twinning and zoned grains are present in subordinate amounts. A few homogeneous grains contain bands of opaques and random included material. Some forsteritic olivine grains are enclosed by thin reaction rims of clinopyroxene and magnetite. The other olivine grains are altered to iddingsite.

TABLE 3. Estimated modes for rock specimens from the Wait Creek Section (in stratigraphic succession).

Sample	Rock Type	Olivine	Augite	Hypersthene	Plagioclase	Felsic Groundmass	Volcanic Glass	Opaques	Hornblende
11-1	Hypersthene Dacite	--	--	15	20	60	--	5	--
11-2	Hypersthene Dacite	--	--	5	15	70	--	10	--
11-3	Hypersthene Dacite	--	--	5	20	70	--	5	--
11-4	Hypersthene Dacite	--	tr	5	25	60	--	10	--
11-5	Hypersthene Dacite	--	--	1	15	81	--	3	--
11-6	Dacite	--	--	--	20	70	--	10	--
11-7	Hypersthene Dacite	--	5	10	18	65	--	2	--
11-8	Hypersthene Dacite	--	--	10	25	60	--	5	--
11-9	Hypersthene Dacite	--	--	7	35	55	--	3	--
2-1	Hypersthene Dacite	--	--	4	70	24	--	2	--
2-2	Hypersthene Dacite	--	--	8	15	80	--	2	--
2-3	Hypersthene Dacite	--	3	4	74	20	--	1	--
2-4	Hypersthene Dacite	--	4	6	59	30	--	1	--
2-5	Augite-Hypersthene Andesite	--	24	8	58	--	9	1	--
2-6	Augite-Hypersthene Andesite	--	19	3	58	--	19	1	--
2-7	Augite-Hypersthene Andesite	--	9	3	78	--	9	1	--
2-8	Augite-Hypersthene Andesite	--	1	2	97	--	--	tr	--
2-9	Augite-Hypersthene Andesite	--	5	--	55	--	40	3	--
2-10	Trachytic Pyroxene Andesite	--	--	tr	93	--	--	6	--
2-11	Basaltic Andesite	1	7	--	50	--	37	5	--
2-12	Augite-Hypersthene Andesite	--	35	5	55	--	4	1	--
2-13	Augite-Hypersthene Andesite	2	33	7	47	--	--	1	--
2-15	Augite-Hypersthene Andesite	--	12	3	59	--	1	25	--
2-16	Dacitic Pyroxene Andesite	--	15	21	63	--	20	1	--
2-17	Augite-Hypersthene Andesite	--	26	5	48	--	--	--	--
2-18	Augite-Hypersthene Andesite	tr	3	4	96	--	--	2	--
2-19	Hornblende-Augite Andesite	--	32	--	59	--	2	1	6
2-20	Hornblende-Augite Andesite	--	28	--	62	--	--	2	8
2-21	Basaltic Andesite	15	--	5	65	--	10	5	--
2-22	Augite-Hypersthene Andesite	--	23	2	84	--	--	1	--
2-23	Augite-Hypersthene Andesite	--	23	3	65	--	7	2	--
2-24	Augite-Hypersthene Andesite	--	6	17	70	--	--	7	--
Lahar-Mudflow, Sedimentary Interbeds									
5-2A	Basaltic Andesite	--	6	3	80	--	10	1	--
3-1	Basaltic Andesite	3	47	--	45	--	--	5	--
3-2	Tholeiitic Basalt	--	37	--	55	--	5	3	--
3-3	Trachytic Pyroxene Andesite	--	24	--	75	--	--	1	--
4-1	Tholeiitic Basalt	--	10	10	60	--	15	5	--
Lahar-Mudflow, Sedimentary Interbeds									
3-4	Tholeiitic Basalt	1	43	5	50	--	--	1	--
3-5	Tholeiitic Basalt	1	12	7	73	--	5	2	--
3-6	Tholeiitic Basalt	--	30	--	45	--	25	--	--
4-2	Tholeiitic Basalt	1	18	7	55	--	10	14	--
Lahar-Mudflow, Sedimentary Interbeds									
4-3	Tholeiitic Basalt	5	12	--	75	--	--	8	--
4-4	Olivine Tholeiite	10	30	--	50	--	4	6	--
4-5	Olivine Tholeiite	15	7	3	70	--	--	5	--

## Andesites

Basaltic andesites and augite-hypersthene andesites are characterized by a coarsely porphyritic texture. Lath-shaped phenocrysts of andesine and microphenocrysts of subhedral hypersthene and anhedral augite occur in an intergranular to pilotaxitic groundmass. The groundmass phases include plagioclase microlites, untwinned feldspar crystallites, orthopyroxene, clinopyroxene, granular magnetite, and light brown volcanic glass. The volume ratio of phenocrysts to groundmass is about 1 : 1. Visually estimated modes are tabulated by rock type for samples of the Wait Creek Section in Table 3 and for the Cabin Creek Section in Table 4.

Plagioclase occurs as the most abundant constituent as well as the dominant phenocrystal phase. Of the total volume it comprises one-half to three quarters of the thin section. The remaining portion, in the absence of volcanic glass, is filled by both orthopyroxene and clinopyroxene. Augite is commonly more abundant than hypersthene. Volcanic glass may occur as a major constituent and appears at the expense of the felsic groundmass phases. Where vesicles are present they may represent from 15% to 30% of the total volume.

Zoning in the plagioclase phenocrysts is oscillatory with cores as calcic as  $An_{52}$  and rims as sodic as  $An_{33}$ . The majority of the plagioclase is homogeneous. A few phenocrysts may contain small amounts of randomly dispersed opaques and birefringent dust. Twinning is according to the carlesbad and carlesbad-albite laws. Augite phenocrysts are sometimes twinned. No zoning was observed in the hypersthene microphenocrysts.

Basaltic andesites exhibit a character transitional between the basalts and the augite-hypersthene andesites. Basaltic andesites have a relatively higher anorthite

TABLE 4. Estimated modes for rock specimens from the Wait Creek Section (in stratigraphic succession).

Sample	Rock Type	Olivine	Augite	Hypersthene	Hornblende	Plagioclase	Volcanic Glass	Opakes	Felsic Groundmass
10-10	Altered Hornblende Dacite	--	--	--	11	20	20	6	43
10-11	Altered Hornblende Dacite	--	--	--	8	30	5	5	62
10-12	Altered Hornblende Dacite	--	4	--	13	20	7	2	65
10-13	Hornblende Pyroxene Dacite	--	4	--	8	25	--	3	50
10-14	Hypersthene-Augite Andesite	--	8	18	--	62	--	12	--
10-15	Altered Hypersthene Dacite	--	3	--	12	39	15	1	30
10-16	Dacitic Pyroxene Andesite	--	5	15	--	47	32	1	--
10-2	Augite-Hypersthene Andesite	--	25	5	--	51	15	3	--
10-3	Pyroxene Dacite	--	3	tr	--	20	--	1	76
10-18	Hypersthene Dacite	--	--	8	--	25	20	3	64
10-19	Hypersthene Dacite	--	--	11	--	53	33	3	--
Lahar-Mudflow Sedimentary Interbeds.									
10-4	Hypersthene-Augite Andesite	--	4	2	--	94	--	tr	--
10-6	Hypersthene-Augite Andesite	--	7	9	--	45	39	1	--
10-20	Pyroxene Dacite	--	5	7	--	84	--	4	--
10-21	Hypersthene-Augite Andesite	--	25	8	--	65	--	2	--
Lahar-Mudflow Sedimentary Interbeds.									
10-22	Pyroxene Andesite	--	25	--	--	72	--	3	--
10-23	Pyroxene Andesite	tr	30	--	--	68	--	2	--
10-24	Hypersthene-Augite Andesite	--	34	5	--	60	--	1	--
10-9	Augite-Hypersthene Andesite	--	35	10	--	53	--	2	--

content of their plagioclases. A more silicious chemical composition is suggested by the appearance of hypersthene. Augite-hypersthene andesites contain both augite and hypersthene as phenocrystal and groundmass phases.

The andesitic dikes are mineralogically similar to the augite-hypersthene andesites. They are sometimes vesicular and tend to have textures that are more diabasic than porphyritic.

### Dacites

The hypersthene and hornblende dacites tend to be moderately porphyritic, containing phenocrysts of stubby, rectangular andesine-oligoclase, and microphenocrysts of hypersthene or hornblende. The groundmass is composed of fine-grained feldspathic material which accounts for three quarters of the volume of the rock. This matrix is composed of microscopic granular grains (quartz?), micro-lites and crystallites of feldspar (some alkali feldspar), crystallites of pyroxene, and granular opaques. Alkali feldspar is not distinguishable optically but by using sodium cobaltinitrite staining techniques its existence was confirmed and may account for as much as one third the total volume of the groundmass in some dacites. Mafic minerals make up less than 20% of the total volume. Where hornblende occurs, augite may also be present. Hornblende is commonly oxidized to brown oxyhornblende and magnetite aggregates are commonly pseudomorphic after the hornblende.

A majority of the plagioclase grains are homogeneous, and twinned according to the carlsbad-albite and albite laws. The stubby plagioclase phenocrysts have a spongy appearance, as they are charged with light brown blebs of volcanic glass. These glass blebs are believed to be caused during partial crystallization

of liquid particles formed by incipient melting of xenocrystic plagioclase along its cleavage traces (Kuno, 1950, p. 968). Many of the plagioclase phenocrysts of both types are enclosed by thin rims of sodic plagioclase.

### Plagioclase Composition of the Flow Units

Tables 5 and 6 list the maximum, minimum, and average anorthite content of phenocrystal plagioclase from the andesite and dacite flows, as well as the twinned plagioclase grains in the basalts. These plagioclase determinations were done by the Rittman Zone Method (Emmons, 1943) as modified for high temperature plagioclase, using the 4-axis universal stage. Where plagioclase microlites were present, their composition was also determined using flat stage techniques (Moorehouse, 1959).

Compositional variance is shown graphically by plotting these maximum, minimum, and average values for each sample in the Wait Creek Section, Figure 5, and the Cabin Creek Section, Figure 6. The dashed line in both figures connects the average value for each specimen in the section. Variance is shown in the difference in average values between successive samples, and in the range within one sample as compared to the range in another sample. Both of these are manifestations of disequilibrium which was probably caused by fluctuating pressure-temperature conditions in the magma during crystallization. For a single sample the average anorthite value approaches the midpoint of the range for that sample. The plagioclase compositional range is relatively greater in andesites than in the dacites or basalts. There appears to be a trend toward increasing sodium content in the average plagioclase composition toward the top of the Wait Creek Section. However, random variation in the average An value between successive samples

TABLE 5. Anorthite content in rocks from the Wait Creek Section  
(in stratigraphic succession).

Sample Number	Range An Phenocrysts	Maximum An Phenocrysts	Average An Phenocrysts	Microlites
11-1	44-33	44	37	-
11-2	44-32	44	38	-
11-3	45-32	45	37	-
11-4	45-33	45	36	-
11-5	44-31	44	36	-
11-6	45-35	45	40	-
11-7	44-32	44	36	-
11-8	46-33	46	37	-
11-9	45-32	45	36	-
2-1	44-30	48	38	-
2-2	44-33	46	38	-
2-3	45-32	46	37	-
2-4	45-32	47	38	-
2-5	48-33	52	46	48
2-6	49-33	50	45	49
2-7	53-32	53	46	49
2-8	46-33	46	38	47
2-9A	53-32	48	39	46
2-10	-	-	-	44
2-11A	48-31	48	39	47
2-12	52-36	52	40	48
2-13	54-32	54	40	46
2-15	48-37	48	45	46
2-16	55-33	55	45	44
2-17	49-28	49	39	43
2-18	56-34	56	46	46
2-19	48-32	48	41	47
2-20	51-30	51	41	46
2-21	54-28	54	37	46
2-22	54-29	54	43	46
2-23	57-32	57	45	46
2-24	50-28	50	37	43
5-2A	55-33	55	38	44
3-1	48-32	48	37	37
3-2	48-36	48	40	-
3-3	-	-	-	44
4-1	52-39	52	47	-
3-4	54-34	54	46	44
3-5	56-37	56	46	39
3-6	43-28	43	33	35
4-2	57-33	52	41	-
4-3	51-38	51	46	-
4-4	58-46	58	53	-
4-5	58-42	58	51	-

TABLE 6. Anorthite content in rocks from the Cabin Creek Section  
(in stratigraphic succession).

Sample Number	Range An Phenocrysts	Maximum An Phenocrysts	Average An Phenocrysts	Microlites
10-10	47-30	47	38	-
10-11	47-32	47	40	-
10-12	46-30	46	38	-
10-13	50-33	50	45	-
10-14	53-30	53	45	44
10-15	54-41	54	47	-
10-16	58-30	58	39	44
10-2	54-33	54	44	44
10-3	47-30	47	37	43
10-18	50-30	50	40	43
10-19	57-28	57	37	46
10-4	48-28	48	36	43
10-6	56-39	56	43	47
10-20	47-29	47	36	47
10-21	56-30	58	32	44
10-22	56-28	56	35	42
10-23	57-37	57	45	47
10-24	51-36	51	40	47
10-9	55-35	55	45	-



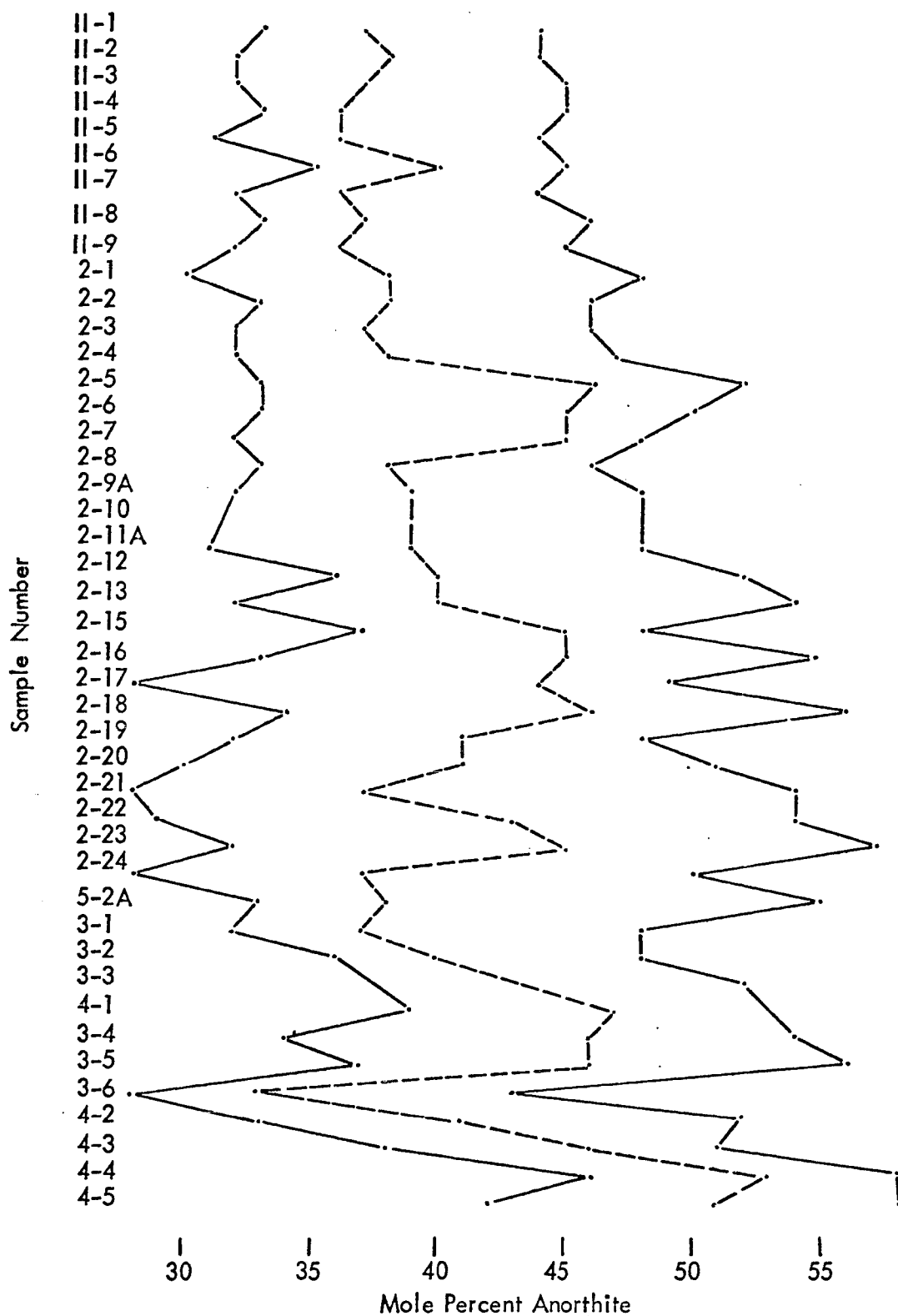


FIGURE 5. Diagram showing the maximum, minimum, and average (dashed line) anorthite content of the plagioclase in the samples from Wait Creek.

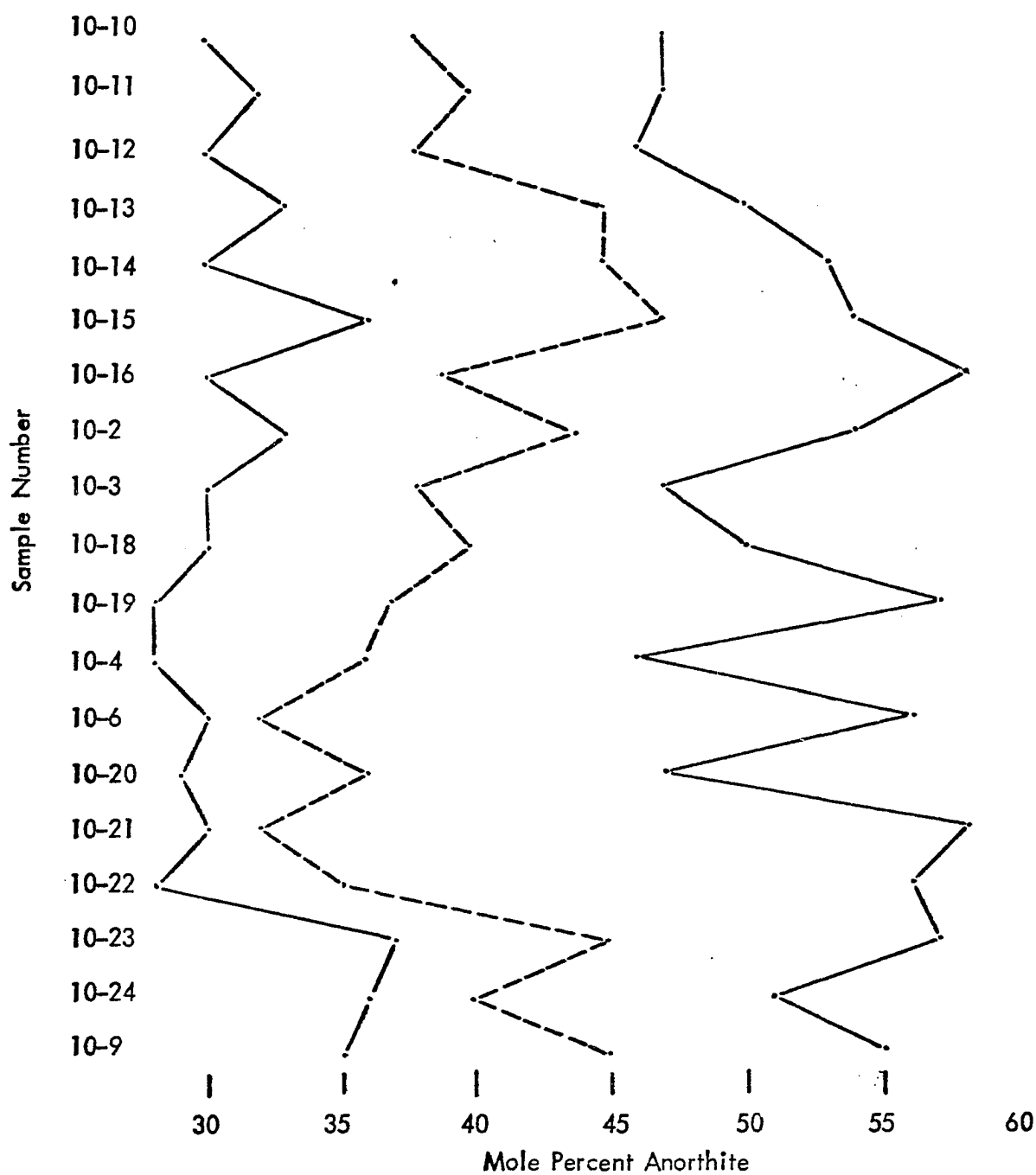


FIGURE 6. Diagram showing the maximum, minimum, and average (dashed line) anorthite content of plagioclase in the samples from Cabin Creek.

compromises the significance of this observation. Alternatively these diagrams may be interpreted as showing a fluctuation about a central An value rather than an enrichment or depletion trend in plagioclase composition up the section.

In an attempt to test the significance of this variation, the standard deviation was computed for the groups basalt, andesite, basalt and andesite, and dacite. The degree of confidence was then established using the t-distribution for small populations and one degree of freedom. The steps followed are outlined in Freund (1967). From these calculations it was determined that the average plagioclase composition for the basalt plus andesite group was significantly different at the 95% confidence level from that in the dacites.

### Chemical Analysis of Rock Units

Table 7 lists the results of flame photometric and spectrophotometric analyses of selected elements in the rock samples from the Wait Creek Section. Precision was checked by performing each elemental analysis three times for each digestion. Replicate samples were prepared and analyzed to check the reproducibility of the results. Except for  $\text{SiO}_2$  determinations, the analytical error in replicate samples is relatively small. The error involved in the silica determinations (5.1 weight percent between replicate samples) may be attributed to analytical technique and sample inhomogeneity at the 0.1 g. level. Variation between replicate analyses for the other elements are as follows: total iron = 0.1 wt.%;  $\text{MgO}$  = 0.26 wt.%;  $\text{Na}_2\text{O}$  = 0.20 wt.%; and  $\text{K}_2\text{O}$  = 0.07 wt.%.

Figures 7a through 7d are diagrams showing the variation in element concentrations in progressively younger flows in the Wait Creek Section. In Figure 7a the configurations of the curves for  $\text{Na}_2\text{O}$  and  $\text{K}_2\text{O}$  are quite similar. Comparisons

TABLE 7. Partial chemical analyses of rock samples from the Wait Creek Section.

Sample Number	SiO <sub>2</sub>	Total Iron as Fe <sub>2</sub> O <sub>3</sub>	MgO	Na <sub>2</sub> O	K <sub>2</sub> O	Total Alkalies
WR 11-1	59.6	3.2	0.5	5.3	1.8	7.1
11-2	59.5	3.0	0.5	5.2	1.8	7.1
11-3	59.6	2.9	0.5	5.2	1.8	7.1
11-4	59.1	2.8	0.5	5.3	1.8	7.2
11-5	59.5	3.2	0.5	5.3	1.9	7.2
11-6	59.5	2.5	0.5	5.4	1.8	7.2
11-7	59.6	3.1	0.5	5.3	1.8	7.1
11-8	60.0	2.8	0.4	5.3	1.8	7.1
11-9	59.1	3.2	0.5	5.4	1.8	7.2
2-1	62.6	3.1	0.7	5.3	1.8	7.1
2-2	64.0	3.2	0.7	5.3	1.9	7.2
2-3	66.5	3.1	0.7	5.3	1.8	7.1
2-4	66.5	3.2	0.6	5.4	1.9	7.2
2-5	56.8	6.3	4.6	4.0	1.0	5.0
2-6	56.8	6.7	4.2	4.0	1.1	5.1
2-7	60.5	6.3	4.4	4.0	1.1	5.1
2-8	66.1	-	-	4.4	1.4	-
2-9A	62.5	5.3	2.3	4.4	1.4	5.8
2-10	62.0	5.9	2.5	4.6	1.3	6.0
2-11A	60.0	5.8	4.0	3.8	1.0	5.0
2-12	60.9	5.5	3.7	4.0	1.2	5.2
2-13	61.0	5.6	3.7	3.9	1.2	5.1
2-15	57.3	5.5	3.9	3.8	1.3	5.1
2-16	59.9	5.5	3.6	4.0	1.2	5.2
2-17	65.0	4.8	2.2	4.2	1.5	5.7
2-18	67.0	4.6	2.4	4.3	1.4	5.7
2-19	59.0	-	-	4.0	1.6	-
2-20	66.1	4.0	2.8	4.6	1.6	6.2
2-21	51.0	-	-	3.6	0.9	-
2-22	52.9	6.2	3.4	4.2	1.3	5.5
2-23	53.3	5.3	3.4	4.2	1.2	5.5
2-24	54.0	5.3	4.2	3.9	1.3	5.2
2-5A	55.0	6.3	3.5	4.0	1.2	5.2
3-1	51.1	6.8	-	5.3	0.6	5.9
3-2	53.8	8.2	2.7	4.4	1.1	5.5
3-3	53.1	8.1	2.4	4.6	1.3	5.8
4-1	-	-	3.9	3.9	1.4	5.2
3-4	54.1	6.2	3.3	4.2	1.1	5.3
3-5	56.8	6.3	3.3	4.1	1.2	5.3
3-6	59.3	5.6	2.7	4.2	1.4	5.6
4-2	54.1	6.0	4.1	3.7	1.4	5.1
4-3	51.6	7.3	>4.2	3.5	0.7	4.2
4-4	52.6	7.2	>4.2	3.6	0.9	4.5
4-5	53.0	7.5	>4.2	3.7	0.9	4.6

of any two sequential samples show that element concentration varies irregularly. Additionally, from one sample to the next where  $K_2O$  shows an increase,  $Na_2O$  may or may not vary sympathetically with this  $K_2O$  increase and vice versa. The andesites and basalts show a marked compositional variation between successive samples whereas the concentrations of  $Na_2O$  and  $K_2O$  in the dacites are quite definitive and show very little change in concentration throughout the sequence, as compared to the variance seen in the basalts and andesites.

Figure 7b shows the  $MgO$  variation in these same samples by a marked departure in composition between the andesite and basalt group and the dacite group. Again, the variation in  $MgO$  concentration between sequential samples in the andesite and basalt groups is unsystematic and wide ranging, whereas  $MgO$  concentrations in the dacites are much lower and show a tight grouping at the 0.6%  $MgO$  level.

Figure 7c defines a pronounced tendency for the younger flows to be increasingly depleted in total iron. Iron concentrations show considerable variation in the andesites and basalts, but less in the dacites.

Figure 7d shows pronounced variation in the  $SiO_2$  content in the andesite and basalt flows as well as the dacites. The upper dacite flow units, however, display less variation in  $SiO_2$  content.

The significant point determined from these diagrams seemed to be the lack, with the exception of total iron, of any systematic compositional variation over the entire section. However, small scale fluctuations about one or more central concentrations, appeared to be related to the basalt, andesite, and dacite groups. To test this hypothesis a step-wise discriminant analysis was performed on the chemical data and the anorthite content of the plagioclase in these same rock samples.

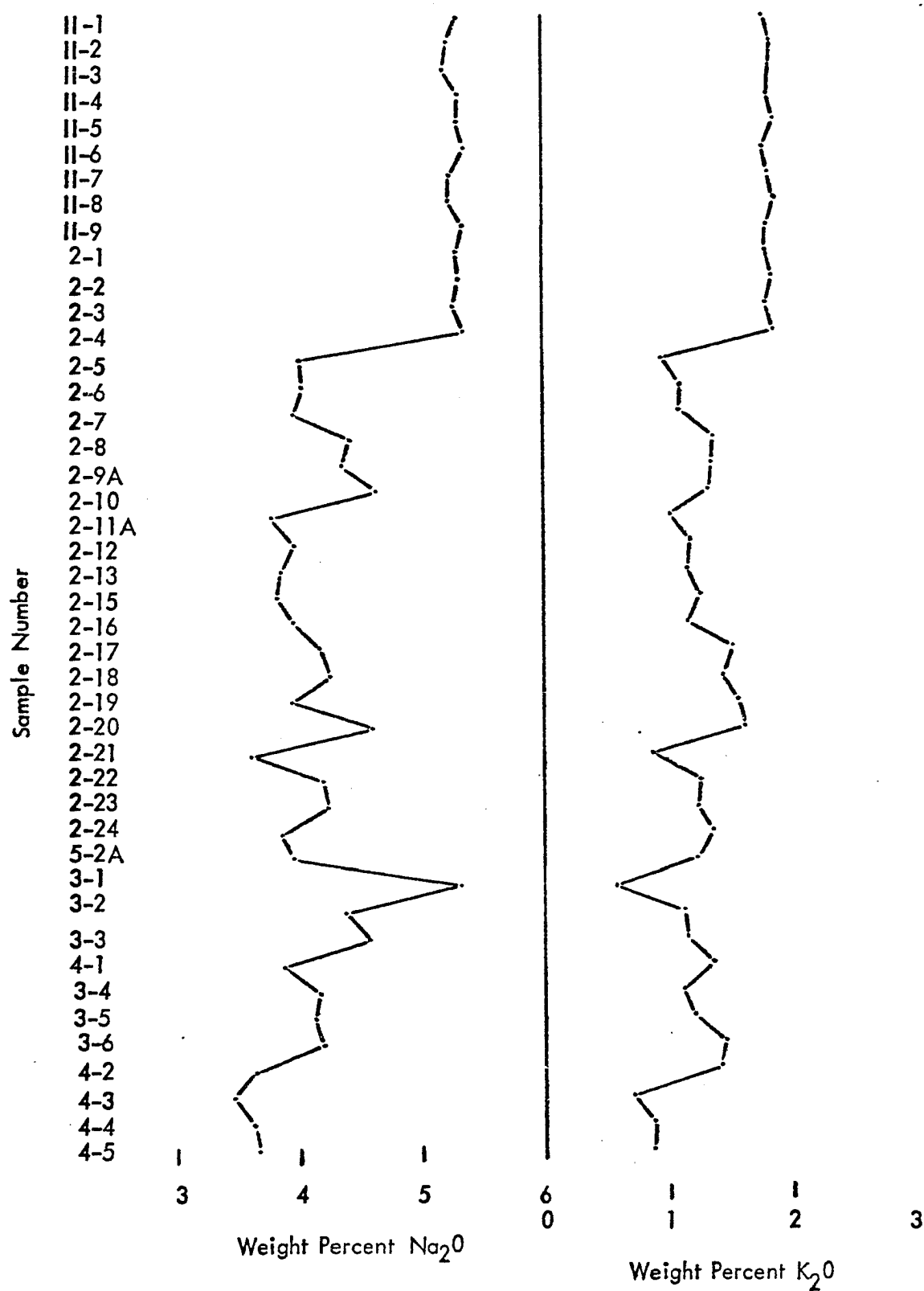


FIGURE 7a. Diagram showing the  $\text{Na}_2\text{O}$  and  $\text{K}_2\text{O}$  variation in rock samples from the Wait Creek Section.

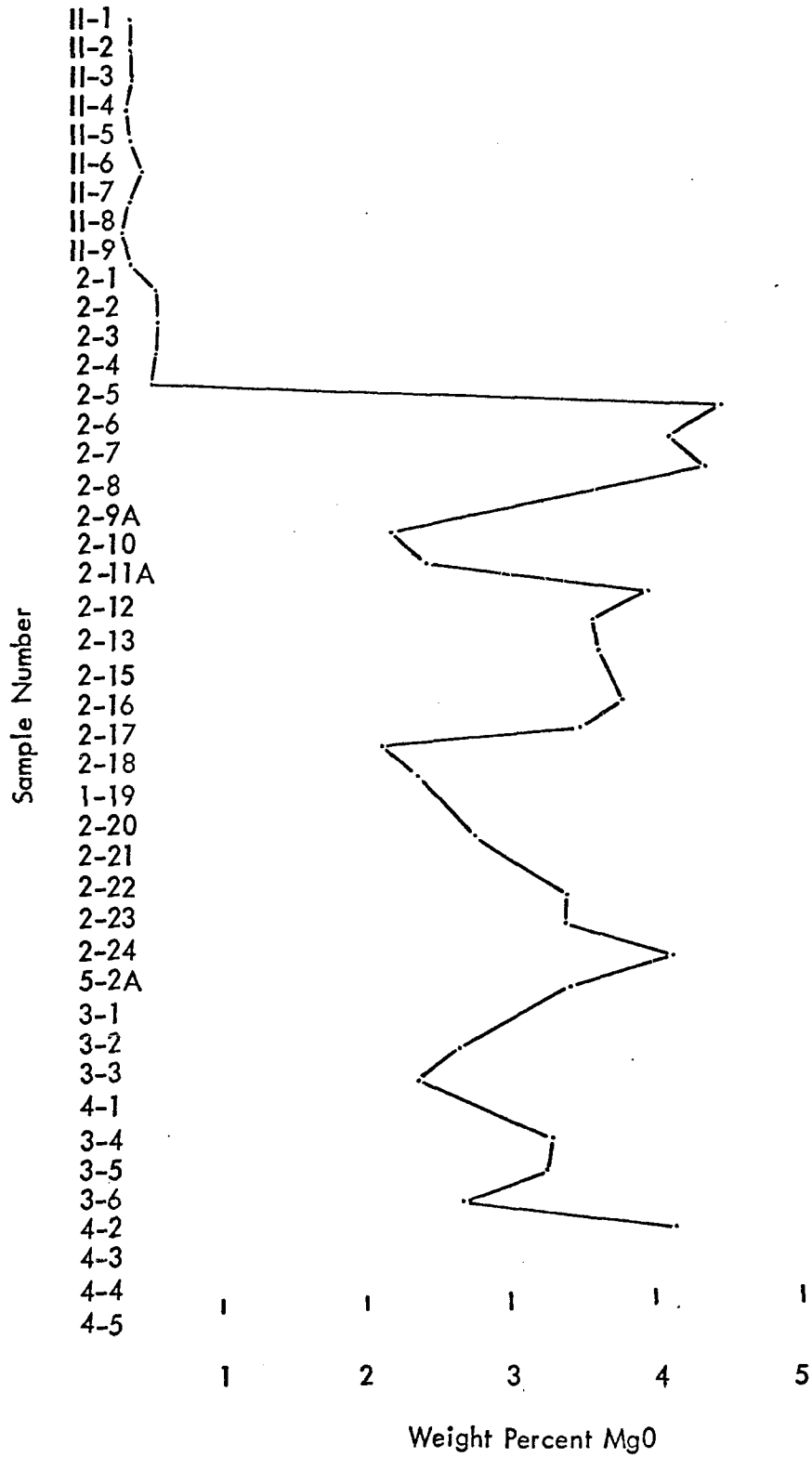


FIGURE 7b. Diagram showing the MgO variation in rock samples from the Wait Creek Section.

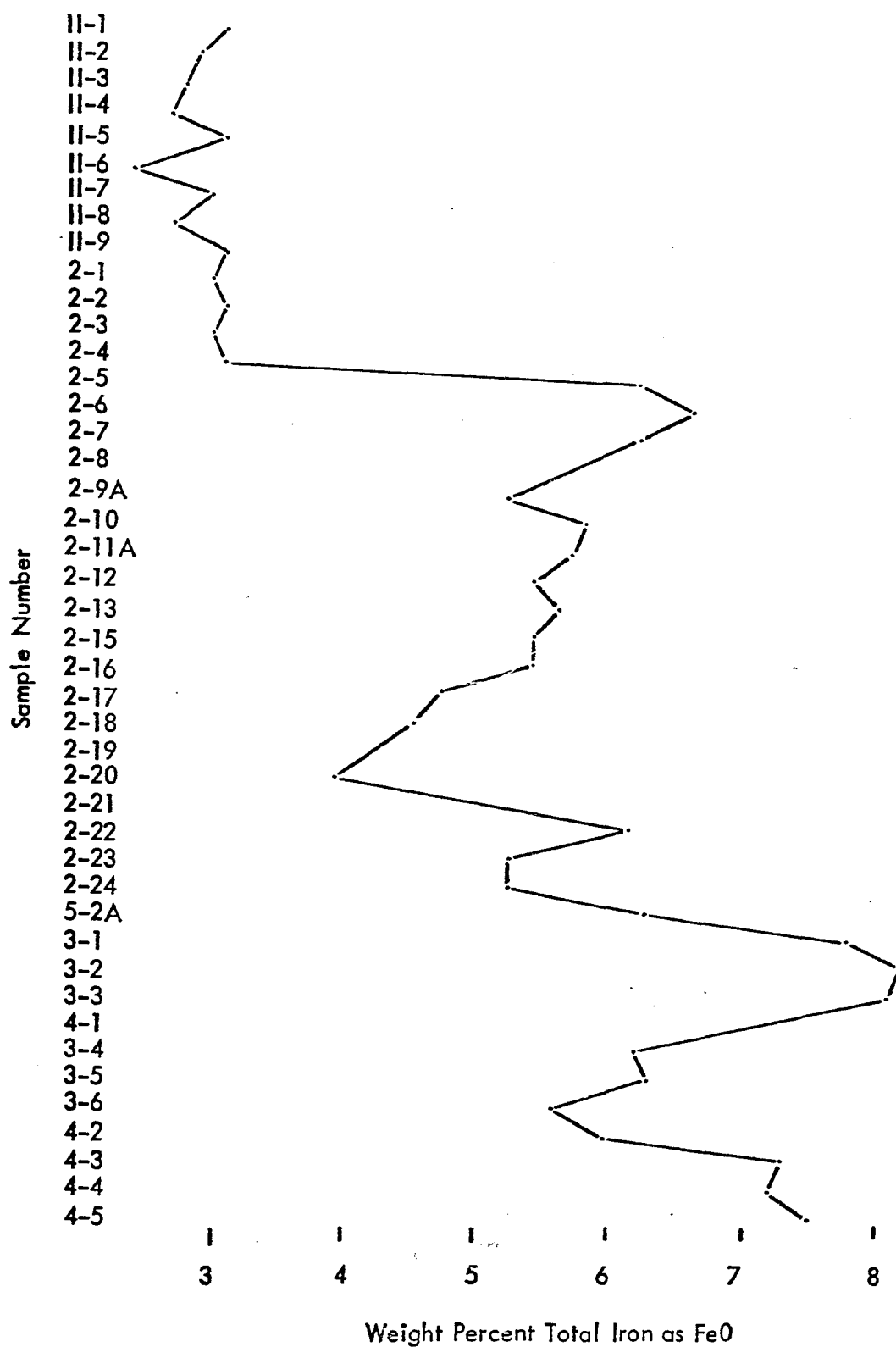


FIGURE 7c. Diagram showing the variation in total iron content of rock samples from the Wait Creek Section.



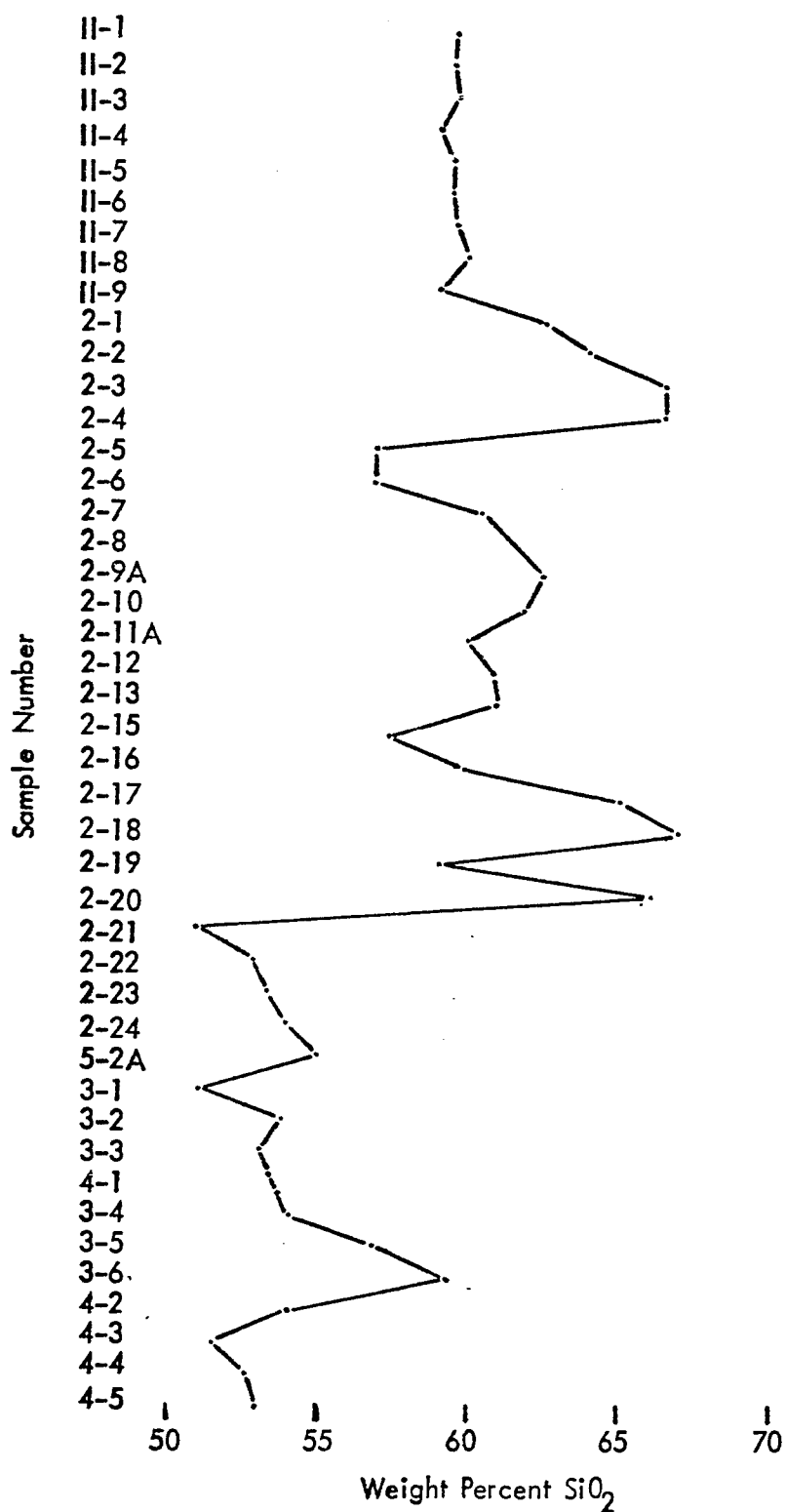


FIGURE 7d. Diagram showing the  $\text{SiO}_2$  variation in rock samples from the Wait Creek Section.

### Stepwise Discriminant Analysis

The stepwise discriminant analysis program (BMD07M, Health Sciences Computing Facility, UCLA, revised July 29, 1968) is a form of multivariate analysis which statistically classifies samples into previously assigned populations on the basis of selected parameters. The chemical data and the compositional determinations of the plagioclase from the rock units in the Wait Creek Section were used as variables to test the statistical reliability of the compositional groups basalt, andesite, and dacite. This method is designed to determine whether an individual really belongs to the assigned group, and not the relative nearness of that individual to the defined population (Reyment, 1966, p. 5).

The discriminant function is a linear combination of the selected variables that most efficiently separates the grouped samples in multidimensional space so that the ratio of between group variance is maximized (Rhodes, 1969, p. 227). This amounts to setting up a series of equations and solving them simultaneously (see Table 8). These calculations define a multidimensional plane that separates 'three dimensional clouds' representing clusters of multivariate observations whose dimensions are defined by the amount of variance within each of the parameters (Davis, 1966, p.2). For three groups, three distances between the centroids of the 'three dimensional clouds' must be considered: the distance between the first and second groups; the distance between the second and third groups; and the distance between the first and third groups (Reyment, 1966, p. 8). This technique is called canonical analysis. This results in the generation of an equation whose coefficients are eigenvectors, derived from eigenvalues. These eigenvalues are obtained from the diagonalization of two component, covariant matrices (see Table 9). This resulting

Table 8. Discriminant Function Table

Variable	Function Dacite	Function Andesite	Function Basalt
An	1.96	2.62	3.20
SiO <sub>2</sub>	5.55	6.53	6.10
Total Iron	45.77	55.34	61.64
MgO	116.80	115.29	116.95
Na <sub>2</sub> O	340.85	286.13	253.15
K <sub>2</sub> O	304.76	329.82	402.20
Constant	- 1491.01	- 1395.28	- 1405.09

TABLE 9. Summary Table

Step Number	Variable Entered Removed	F Value to Enter or Remove	Number of Variables Included
1	K <sub>2</sub> O	210.62	1
2	Na <sub>2</sub> O	5.03	2
3	Total Iron	4.22	3
4	SiO <sub>2</sub>	3.68	4
5	An	0.94	5
6	MgO	0.14	6

Variable	Eigenvalues	Cumulative Proportion of Total Dispersion	Canonical Correlations
An	19.79	0.97	0.98
SiO <sub>2</sub>	0.65	1.00	0.63
Total Iron	0.00	1.00	0.01
MgO	-0.00	1.00	0.00
Na <sub>2</sub> O	-0.00	1.00	0.00
K <sub>2</sub> O	-0.00	1.00	0.00

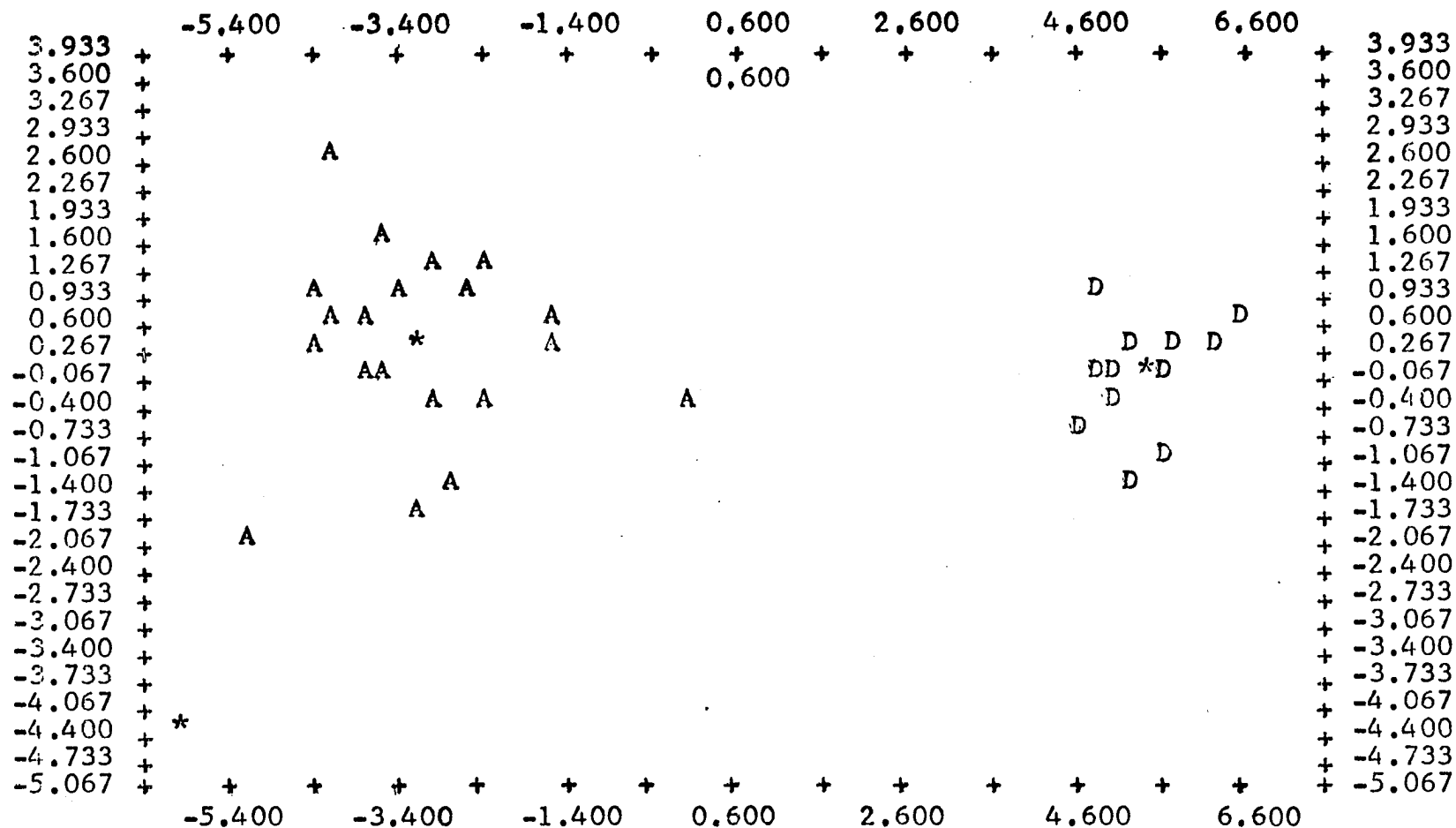


FIGURE 8. Plot of first and second canonical variables showing the separation of dacites (D) from andesites (A). The single basalt analyzed is represented by the \* in the lower left hand corner of the graph, the \* indicates group means.

equation can then be solved in terms of canonical variables for each individual sample. These variables, in the form of x and y coordinates, are then plotted by the computer on a two dimensional grid designed to show the 'separation' of the defined groups (see Figure 8).

The results of this analysis indicate that the dacite group is compositionally distinct from the andesites and basalts, but that the andesite and basalt groups are compositionally convergent, and possibly gradational. The entire program was run two additional times; 1) using the variables,  $\text{SiO}_2$ ,  $\text{FeO}$ ,  $\text{Na}_2\text{O}$ , and  $\text{K}_2\text{O}$ , and 2) the most distinctive variable,  $\text{Na}_2\text{O}$ . The resulting plots for the additional runs closely resembled those of the first run using six variables.

#### Variation Diagrams

Figure 9 shows the variation of selected oxides with increasing  $\text{SiO}_2$  content, in rock samples from the Wait Creek Section. The total iron content decreases markedly with increasing  $\text{SiO}_2$  in the basalts and andesites. The plots of the basalts are grouped at the low silica end of the trend. The dacite plots define a separate and distinct compositional field, and show a small variation in iron content with increasing  $\text{SiO}_2$  concentration. The  $\text{MgO-SiO}_2$  diagram shows similar relations for the dacites though the decrease in  $\text{MgO}$  with increasing  $\text{SiO}_2$  for the andesites and basalts is not as steep as the iron depletion trend. Again the dacites form a distinct compositional grouping with little variation in  $\text{MgO}$  concentrations over a rather wide range in  $\text{SiO}_2$  concentrations. In the  $\text{Na}_2\text{O-SiO}_2$  and  $\text{K}_2\text{O-SiO}_2$  diagrams, the trend appears to favor a slight enrichment in  $\text{K}_2\text{O}$  and  $\text{Na}_2\text{O}$  with increasing  $\text{SiO}_2$ . The dacite plots again form a group defining nearly constant  $\text{Na}_2\text{O}$  and  $\text{K}_2\text{O}$  concentrations regardless of silica content. The actual alkali content of the dacites

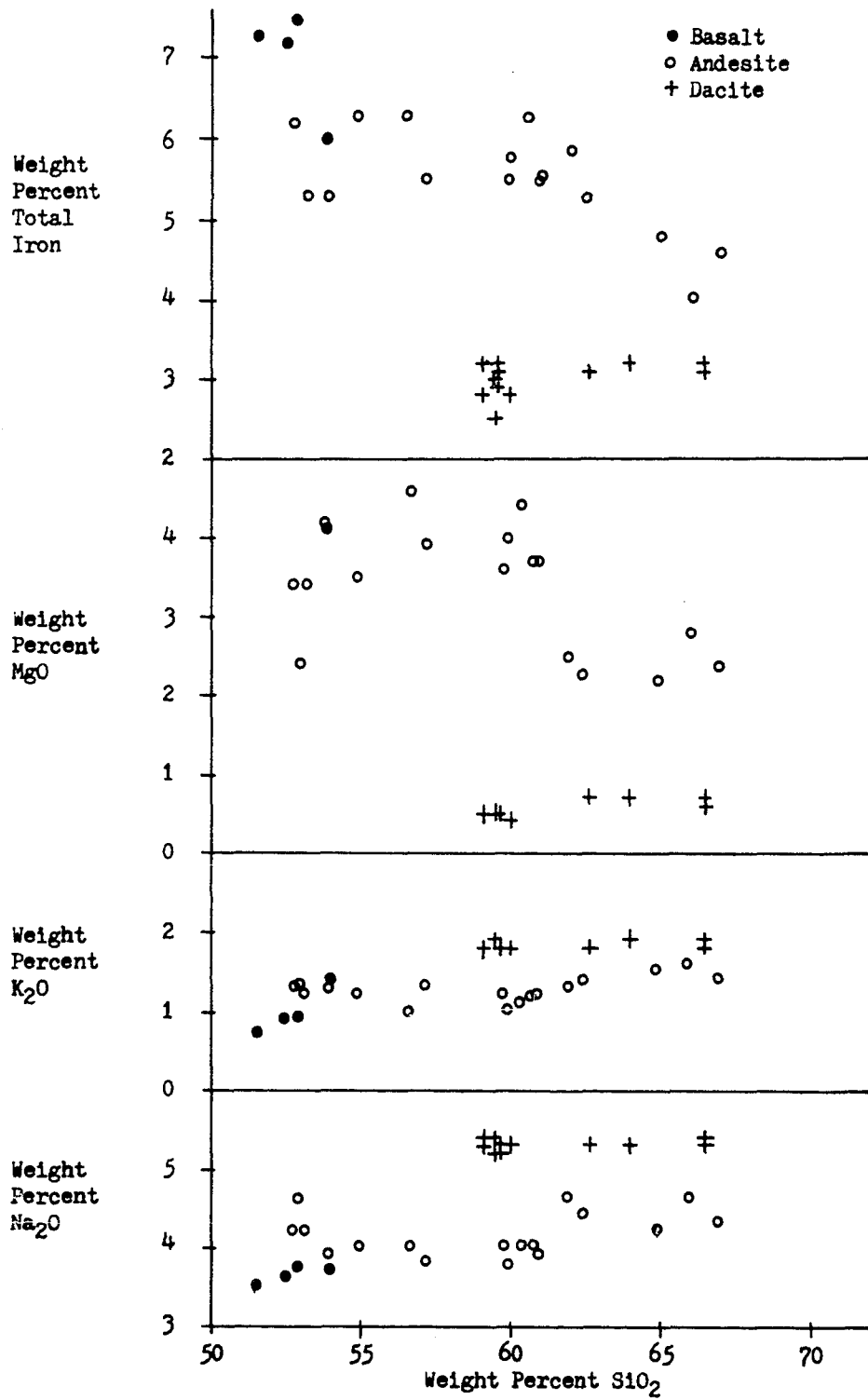


FIGURE 9. Silica variation diagrams for analyzed rock samples from the Wait Creek Section.

however, is only slightly more than that in the andesites and basalts. It should be noted that the dacites do not plot along the trends defined by data for the andesites and basalts, but plot as high alkali analogues of the more silicious andesites.

Figure 10 shows the variation of total alkalis with increasing  $\text{SiO}_2$  for the analyzed rocks. Kuno (1965) has statistically subdivided this diagram into the three compositional fields as shown. The significance of the alkali and pigeonitic series has been discussed in Chapter III. The high alumina series is thought to represent a transition between the two basalt types, due to late crystallization of the plagioclase in the parental melt (Kuno, 1960). In this diagram plots of the analyzed Wrangell volcanics form a broad band of scattered points across the high alumina basalt field with the basalts being at the low silica end of the field. In this diagram the dacites appear to be alkali-rich analogues of the augite-hypersthene andesites.

The FMA diagram shown as Figure 11 compares the compositional trends of the Wrangell volcanics to the principle differentiation trends of classically important rock suites. The plots representing the Wrangell volcanics in this diagram appear to have a bimodal rather than linear distribution. The usual differentiation trends do not fit the data closely. It should be noted that the tholeiitic basalts of the Nabesna District are slightly richer in total alkalis than typical tholeiites as usually defined on FMA diagrams.

### Paragenesis

The mineralogy of the volcanic rocks from the Wait Creek and Cabin Creek sections suggests a crystallization sequence that follows Bowen's reaction series.

The sequence outlined by Bowen is only slightly modified by changes in composition



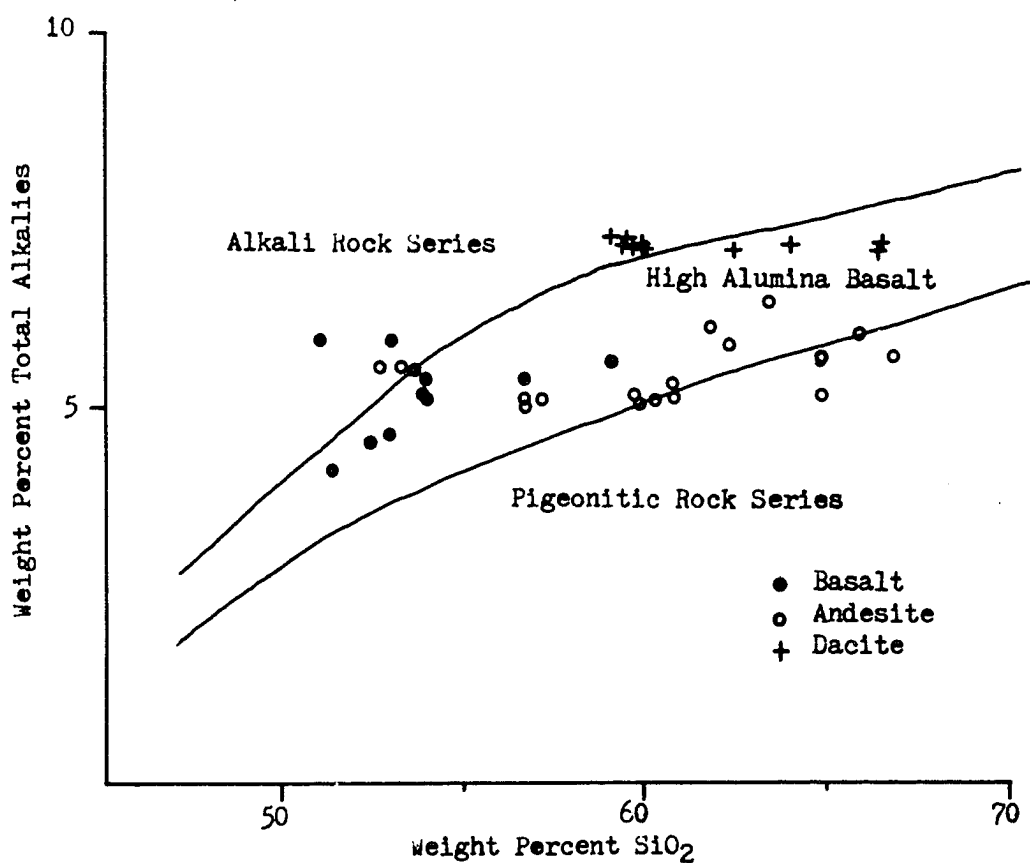


FIGURE 10. Diagram showing the variation of total alkalies with increasing  $\text{SiO}_2$ . Compositional fields taken from Kuno (1965).

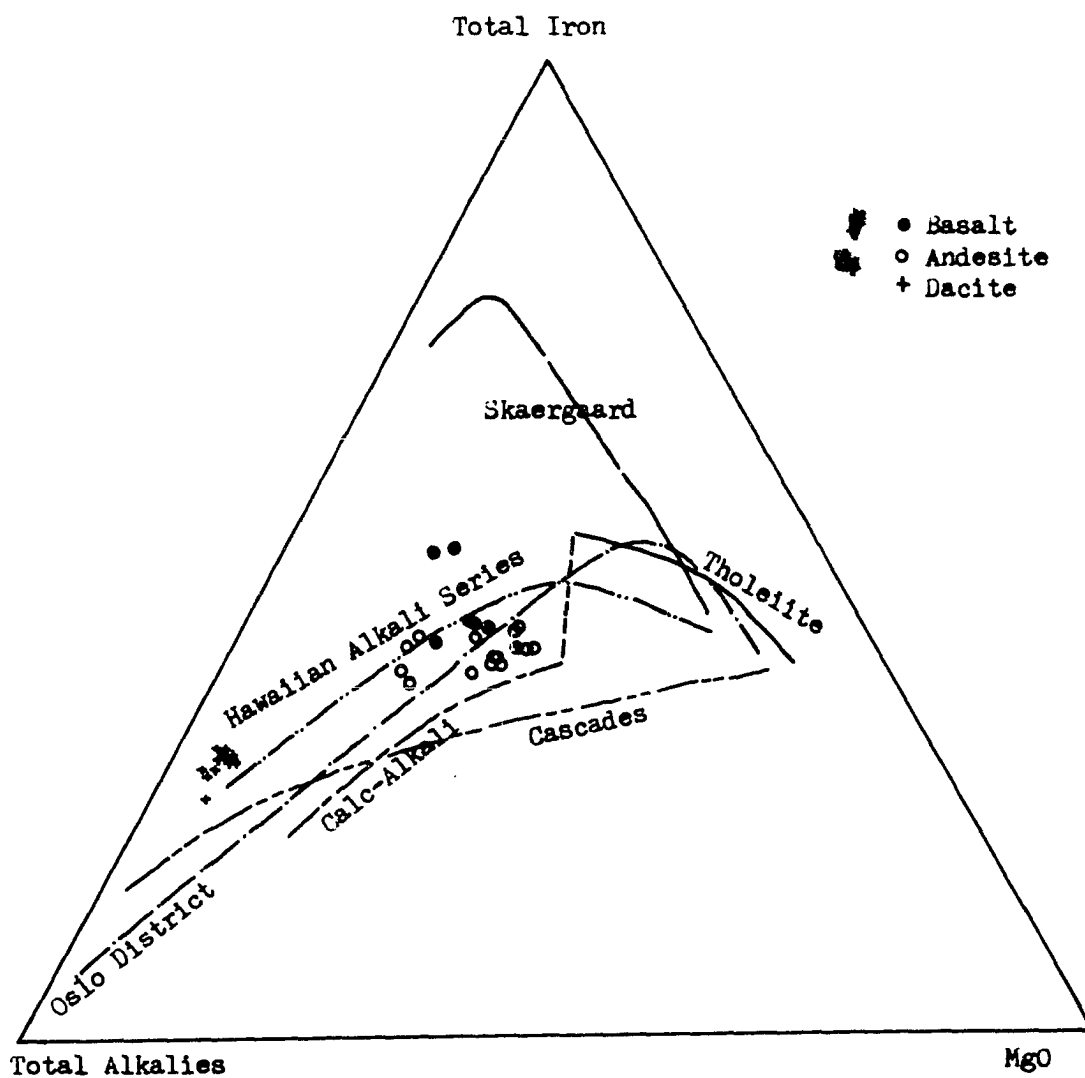


FIGURE 11. FMA triangular diagram showing plots of analyzed rock samples from the Wait Creek Section. Differentiation trends taken from Yoder and Tilley, 1962, page 424.

of the initial melts, intratelluric crystallization, viscosity, and volatile content.

Olivine was the first major constituent to begin crystallizing in the basalts.

In the more silicious andesites and dacites olivine did not form, or formed unstably and was quickly reabsorbed. In these more silicious members, crystallization begins later in the sequence with pyroxene and plagioclase. In the basalts olivine crystallization may have begun before extrusion as judged by the porphyritic character of the euhedral olivine. A few of these grains show rounding, presumably by magmatic corrosion. The composition of these olivine grains is forsteritic whereas the groundmass occurrence of olivine in the basaltic andesites is richer in the fayalite component. This more iron rich olivine must have crystallized after pyroxene, from a liquid depleted in magnesium and silica as a result of earlier pyroxene crystallization.

Hypersthene was the next constituent to begin crystallizing, and was quickly followed by the simultaneous crystallization of augite and plagioclase. Subhedral hypersthene is sometimes surrounded by augite rims in the basalts. It also typically occurs as a phenocrystal phase in the andesites. Augite occurs in both the phenocrystal and groundmass modes in the andesites, and maintains its euhedral character in all the rock types where it occurs. An occasional included grain of augite is observed in the plagioclase laths in the augite-hypersthene andesites.

Hornblende, which chiefly occurs in the dacites of the Cabin Creek Section, presumably crystallized after pyroxene crystallization had commenced in an environment characterized by high partial water pressure. The hornblende phenocrysts are now oxidized, and in some cases magnetite has formed pseudomorphic aggregates after the hornblende. This oxidation occurred late in the crystallization history

of the rocks, as a result of the release of volatiles during extrusion.

The wide range in anorthite content of the plagioclase and the simple oscillatory zoning indicates disequilibrium between the crystals and the magma. This zoning is better developed in the andesites, and probably reflects changes in the volatile content of the melt, or possible vertical movement of magma in the vent during crystallization. The porphyritic nature of the andesites and dacites is generally attributed to intratelluric crystallization or contamination by non-cognate xenocrysts. The plagioclase phenocrysts of the andesites are considered to be cognate as the average phenocrystal plagioclase composition is similar to that of the plagioclase microlites.

The abundance of microcrystalline, felsic groundmass in the dacites probably reflects the high viscosity of the melt. A highly viscous medium slows crystallization reactions. The later phases of Bowen's reaction series, alkali feldspar and quartz, that would have formed under slower cooling conditions were quenched and locked in as occult phases in the glassy portions of the groundmass. Magnetite occurs in the glassy and groundmass modes of the three rock types but is explained as having formed late from a melt depleted in iron. Alkali feldspar is present in the dacites as microcrystalline grains and crystallites. Modal quartz was found only in one sample, WR 2-18, and then only as a trace constituent.

---

## CHAPTER VI

### SUMMARY AND CONCLUSIONS

- 1) The Wrangell volcanics in the Nabesna District comprise a sequence of andesitic lava flows nearly 4000 feet thick which unconformably overlies older Tertiary and Triassic rocks.
- 2) The oldest flows of the Wait Creek Section are at least  $13.5 \pm 0.8$  m.y. old as determined by a whole rock  $K^{40}/Ar^{40}$  radiogenic date.
- 3) The rock types in the Wait Creek Section occur in the chronological sequence; 1) tholeiitic basalts, 2) augite-hypersthene andesites, and 3) hypersthene dacites.
- 4) The relative abundance of these three rock types may be expressed volumetrically as follows:

Tholeiitic Basalt . . . . .	13%
Pyroxene Andesite . . . . .	59%
Hypersthene Dacite . . . . .	28%
- 5) The associated rock types, orogenic setting, mineralogy, and chemical composition of the flow units indicates that the Wrangell volcanics belong to the calc-alkali rock series.
- 5) Diagrams showing sequential changes in element concentration show an unsystematic variation, but delineate compositional fields which correspond to rock type. The dacites form a distinct group in the variation diagrams and are quite separate from the andesite and basalt fields. Compositional variation is generally greater in the basalts and andesites than for the dacites.
- 7) Multivariate discriminant analysis using plagioclase composition and chemical data shows that, for the predetermined groups, dacite is indeed a distinct population when compared to the andesites and basalts. Further, the chemical and mineralogical

similarity of the basalts and andesites suggests that the two types are genetically interrelated.

8) Standard variation diagrams show these same groupings quite well, in addition to the trends generally considered characteristic of calc-alkali andesitic volcanism. All three diagrams show a bimodal distribution of rock type into the compositional fields of basalt - andesite, and dacite.

9) The basalts and andesites form a single, moderately defined trend in the silica variation diagrams and alkali-silica variation diagram. The basalts are located at the low silica end of the trend. The dacites, however, form a separate and distinct trend which is unrelated to the basalt plus andesite trend.

10) The scatter of data points on the FMA variation diagram does not define a linear trend but rather a bimodal, compositional distribution of basalt-andesite and dacite which does not seem to be closely related to the usual differentiation trends.

11) The Wrangell volcanics were probably derived by partial melting of the lower crust at various depths to form batches of magma in which fractional crystallization may have occurred to a limited extent.

### The Wrangell Volcanics and Andesite Theory

Though the three associated rock types occur in the succession basalt, andesite, dacite, several factors argue against a straight magmatic differentiation by fractional crystallization. The abundance of andesite over the combined volume of the other rock types is contrary to the expected exponential decrease in relative volumes of the fractionated rock types originating from a primary basalt parent. The anorthite content of the plagioclase does not show any uniform trend to suggest that the successive flows are related by fractional crystallization. Likewise the partial

chemistry of the succession presents a complex picture and not the linear enrichment and depletion trends considered to be characteristic of fractional crystallization.

Assimilation of large volumes of host rock by a primary magma would require the magma to be considerably hotter than the temperature at which it would normally begin to crystallize. It is due to this 'superheat' restriction that many petrologists object to assimilation as a major factor in magmatic differentiation. Evidence such as non-cognate phenocrysts or xenoliths, indicative of assimilation, were not observed in the basalt and andesite flows, consequently assimilation of sialic material by a parental basalt magma is not likely to have produced the Wrangell volcanics.

A primary andesite source does not completely explain the observed data either. Basalt cannot be derived from a magma of a more felsic composition. To derive the observed flows by this mechanism would require at least two parental magmas and then still have to account for the derivation of these two parents of different composition.

The simplest explanation which best fits the data is that some sort of 'batch' mechanism has been operating to produce the observed succession. Partial melting of the lower crust or upper mantle places no restriction on sequence of occurrence of rock type, strict uniformity of composition, relative volume of rock types, defined trends in mineralogic composition, or bulk chemistry among the rock types.

The similarity of the average composition of the earth's crust to that of the average andesite makes it theoretically possible to completely melt crustal material and produce a melt of andesitic composition and partial melting could produce magmas of a more felsic composition. Green and Ringwood (1969), presuming the upper

mantle to be quartz eclogite, have shown experimentally that partial melting of this quartz eclogite at depths ranging from 80 to 150 km can produce magmas of the composition of any of the members of the calc-alkaline suite. Uffen (1959) proposed that pressure release occurring at an earthquake focus could melt the surrounding rock if the rock were close to its melting temperature and under high confining pressure. The proximity of the Wrangells to two major Tertiary-Quaternary strike slip faults, the Wrangell's tectonic setting, as well as their location across the trend of major earthquake epicenters (Stone, 1968, p. 437, Fig. 2), allow this as a reasonable explanation for the origin of the Wrangell volcanic succession.

#### Recommendations for Further Work

Subsequent work on the Wrangell volcanics should include additional field and laboratory study. To obtain representative samples of the flows as well as a better understanding of the complex field interrelationships, the study and sampling of at least one additional section is necessary. Tracing recognizable marker horizons between the sections is also essential to a better understanding of the stratigraphy. Laboratory work should additionally include whole rock silicate analyses, and chemical analyses for selected elements by rapid analytical techniques. Trace element and constituent mineral phase analysis should also be included in this program. Critical rock units should be dated by  $K^{40}/Ar^{40}$  radiogenic dating techniques.

Whole rock analyses are needed for classification, the comparative study of the various rock types, and to provide checks on the accuracy of the chemical analysis by rapid analytical methods. Precise chemical analyses of the separated mineral



phases could be used to delineate significant compositional differences in the ground-mass and phenocrystal phases of the same mineral.

Systematic minor and trace element analyses should be acquired through emission spectrographic and x-ray fluorescence techniques. These data, including determinations of Sr, Rb, Ba, Na, K, Zr, Ti, U, Th, La or Ce, Ni, Co, and Mn could be used to determine whether the volcanics originated from a single magma type or separate magma batches. The trace element determinations for Sr, Zr, Rb, Ba, Ti, and Mn should also aid in the correlation of units in the various sections. A study of trace element abundances in the successive flow units should provide some insight into the processes operating throughout the eruptive history.

For example, low K/Rb and high Ba/Sr cation ratios are attributed to fractional crystallization in magmas, whereas a high Ba/Rb ratio is typical of unfractionated material (Taylor and White, 1966). These authors also consider the highly charged large cation ratio, Th/U, to be a function of the depth at which andesitic melts originate. Ferromagnesian element ratios such as Ni/Co are also important. In this case the ratio is believed to indicate whether or not high potassium andesites are derived from normal andesites by the simple addition of potassium.

The final phase of this investigation should include the dating of selected rock units to provide an absolute time frame for the geochemical and petrological studies.

## REFERENCES CITED

- Bailey, E. B., and others (1924), Tertiary and post-Tertiary geology of Mull, Loch Aline and Oban. Mem. Geol. Surv. Scotland, cited in Tilley, C. E. (1950). Some aspects of magmatic evolution. Quart. Jour. Geol. Soc. London, Vol. 106, p. 37-61.
- Bargar, W. R. A., and A. M. Goodwin (1969), Andesites and Archean volcanism of the Canadian Shield, in Proceedings of the andesite conference, McBirney, A. R. (ed.), p. 121-150.
- Benioff, H. (1964), Orogenesis and deep crustal structure: Additional evidence from seismology. G.S.A. Bull., Vol. 65, p. 385-400.
- Bingham, D. K. (1967), Ice motion and heat flow studies on Mount Wrangell, Alaska. Unpublished MS thesis, University of Alaska, 117 p.
- Black, R. F. (1958), "The Wrangell Mountains" in Landscapes of Alaska. Williams, H. (ed.), University of California Press, Berkeley, p. 30-33.
- Bowen, N. L. (1928), The evolution of igneous rocks. Princeton University Press, New Jersey, 332 p.
- Brew, D. A., L. J. P. Muffler, and R. A. Loney (1969), Reconnaissance Geology of the Mount Edgumbe volcanic field, Kruzof Island, Southeastern, Alaska. U.S.G.S. Prof. Paper 650-D, pp. D-1-D-18.
- Capps, S. R. (1916), The Chisana-White River District, Alaska. U.S.G.S. Bull. 630, 126 p.
- Chayes, F. (1964), A petrographic distinction between Cenozoic volcanics in and around the open oceans. J.G.R., Vol. 69, p. 1573-1588.
- Davis, J. C. (1966), Programming the discriminant classification function for small computers, in Merriam, D. F. (ed.) Computer applications in the earth sciences. p. 1-4.
- Denton, G. H. (1969), Miocene and Pliocene glaciations in Southern Alaska. Am. Jour. Sci., Vol. 267, p. 1121-1142.
- Denton, G. H. and R. L. Armstrong (1969), Miocene-Pliocene glaciations in Southern Alaska. Am. Jour. Sci., Vol. 267, No. 10, p. 1121-1142.
- Dickinson, W. R. (1967), Andesitic volcanism and seismicity around the Pacific, Science, Vol. 157, p. 801-803.

- Dickinson, W. R. (1968), Circum-Pacific andesite types, *J. G. R.*, Vol. 73, p. 2261-2269.
- Emmons, R. C. (1943), The Universal Stage. *G.S.A. Memoir No. 8*, p. 115-134.
- Forbes, R. B., Ray, D. K., Katsura, T. and others (1969), The comparative chemical composition of continental vs. island arc andesites in Alaska, in Proceedings of the andesite conference, McBirney, A. R. (ed.) p. 111-120.
- Freund, J. E. (1967), Modern elementary statistics. (3rd ed.) Prentice Hall, Inc., Englewood Cliffs, New Jersey, p. 225-227, and Table II p. 383.
- Furst, J. I. (1968), Reconnaissance petrology of the andesites of the Mr. Wrangell caldera, Alaska. Unpublished MS thesis University of Alaska, 83 p.
- Gorshkov, G. S. (1969), Geophysics and petrochemistry of andesite volcanism in the circum-Pacific belt, in Proceedings of the andesite conference, McBirney, A. R. (ed.), p. 91-98.
- Grantz, A. (1966), Strike slip faults in Alaska. U.S.G.S. Open file report, 82 p.
- Green, T. H., and A. E. Ringwood (1969), High pressure experimental studies on the origin of andesite, in Proceedings of the andesite conference, McBirney, A. R. (ed.), p. 21-64.
- Griffiths, J. C. (1966), Application of discriminant functions as a classification tool in the geosciences. In Merriam, D. F. op. cit., p. 48-52.
- Hess, H. H. and A. Poldervaart (1967), Basalts two vols. Wiley Interscience, New York, 862 p.
- Ingemells, C. O. (1962), Determination of major and minor alkalies in silicates by differential flame spectrophotometry. *Talanta*, Vol. 9, pp. 781-793.
- Isacks, B., J. Oliver, and L. R. Sykes (1968), Seismology and the new global tectonics, *J.G.R.*, Vol. 73, p. 5855-5899.
- Jack R. N. and I. S. E. Carmichael (1968), Chemical finger-printing of acid volcanic rocks. Calif. Div. of Mines and Geology, SR100, pp. 17-32.
- Kennedy, W. Q. (1933), Trends of differentiation in basaltic magmas. *Am. Jour. Sci.*, Ser. 5, Vol. 25, p. 239.
- Kerr, P. F. (1959), Optical Mineralogy. McGraw Hill Book Co., Inc., New York, 442 p.

- Kuno, H. (1936), On the crystallization of pyroxenes from rock magmas with special reference to the formation of pigeonite. In Selected papers by Hisashi Kuno (1969) Geol. Inst. Univ. of Tokyo, p. 107-116.
- Kuno, H. (1950), Petrology of Hakone Volcano and the adjacent area, Japan. GSA Bull. Vol. 61, p. 958-1014.
- Kuno, H. (1953), Formation of calderas and magmatic evolution. Trans. Am. Geop. Union, Vol. 37, p. 267-280.
- Kuno, H. (1959), Origin of Cenozoic petrographic provinces of Japan and surrounding areas. Bull. Volc., Ser. 2, Tome XX, p. 37-76.
- Kuno, H. (1965), Fractionation trends of basalt magmas in lava flows. Jour. Pet. v. 6, p. 302-321.
- Kuno, H. (1969), Andesites in time and space, in Proceedings of the andesite conference, McBirney, A. R. (ed.), p. 13-20.
- Kuno, H. (1969), Selected papers by Hisashi Kuno Geological Institute, University of Tokyo, Japan, 886 p.
- MacDonald, G. A. (1944), Unusual features in ejected blocks at Kilauea volcano. Am. Jour. Sci., Vol. 242, p. 322.
- MacDonald, G. A. (1960), Dissimilarity of continental and oceanic rock types. Jour. Pet., Vol. 1, p. 172-177.
- MacKevett Jr., E. M. (1963), Preliminary geologic map, McCarthy C-5 Quadrangle, Alaska. U.S.G.S. Misc. Invest. Map 1-406.
- MacKevett Jr., E. M. (1970), Geology of the McCarthy B-4 quadrangle, Alaska. U.S.G.S. Bull. 1333, 31 p.
- McBirney, A. R. (ed.) (1969), Proceedings of the andesite conference. International Upper Mantle Project Scientific Report No. 16, State of Oregon, Department of Geol. and Mineral Industries, 193 p.
- Mendenhall, W. C. (1905), Geology of the Central Copper River Region, Alaska. U.S.G.S. Prof. Paper 41, p. 54-62.
- Mendenhall, W. C. and F. C. Schrader (1903), The mineral resources of the Mt. Wrangell District, Alaska. U.S.G.S. Prof. Paper 15, 71 p.
- Moffit, F. H. and R. G. Wayland (1943), Geology of the Nutzotin Mountains and gold deposits near Nabesna, Alaska. U.S.G.S. Bull. 933-B, p. 103-162.

- Moffitt, F. H. (1954), Geology of the eastern part of the Alaska Range and adjacent area. U.S.G.S. Bull. 989-D, 148 p.
- Pewe, T. L., D. M. Hopkins, and J. L. Giddings (1965), The Quaternary geology and archaeology of Alaska in The Quaternary of the United States. Wright and Frey (eds.), p. 355-374.
- Raleigh, C. B. and W. H. K. Lee (1969), Sea floor spreading and island arc tectonics, in Proceedings of the andesite conference., p. 99-110.
- Ray, D. K. (1967), Geochemistry and petrology of the Mt. Trident andesites in Katmai National Monument. Unpublished Ph.D. dissertation, University of Alaska, 198 p.
- Reyment, R. A. (1966), Homogeneity of covariance matrices in relation to generalized distances and discriminant functions. In Merriam, D.F. op. cit., p.5-9.
- Rhodes, J. M. (1969), The application of cluster and discriminatory analysis in mapping granite intrusions. *Lithos* v. 2, p. 223-237.
- Richter, D. H. and N. A. Matson, (1971), Quaternary faulting in the Eastern Alaska Range. *GSA* v. 82, p. 1529-1540.
- Rosenbush, H. (1923), *Elemente der gesteinslehre.*, 4th ed. Stuttgart, Germany.
- Smith, P. S. (1939), Areal geology of Alaska. U.S.G.S. Prof. paper 192, 100 p.
- Stone, D. B. (1968), Geophysics in the Bering Sea and surrounding areas: A review, *Tectonophysics*, Vol. 6, p. 433-460.
- Taylor, S. R. and A. J. R. White (1966), Trace element abundances in andesites. *Bull. Volc.*, Vol. 29, p. 177-194.
- Taylor, S. R. (1969), Trace element chemistry of andesites and associated calc-alkaline rocks, in Proceedings of the andesite conference, McBirney, A. R. (ed.), p. 43-63.
- Tilley, C. E. (1950), Some aspects of magmatic evolution. *Quart. Jour. Geol. Soc. London*, Vol. 106, p. 37-61.
- Tomata, T. (1932), Geological and petrological study of Dogo, Oki, Part XX, *Jour. Geol. Soc. Tokyo*, Vol. 34, p. 675.
- Troger, W. E. (1956), Optische bestimmung der gesteinsbildenden minerale. Teil 1, auf 1, E. Schwiz Verlags, Stuttgart, p. 111.
- Turner, F. J. and J. Verhoogen (1960), *Igneous and metamorphic petrology.* McGraw Hill Book Co. Inc., New York, 694 p.

- Uffen, R. J. (1959), The origin of rock magma. J.G.R., Vol. 64, p. 117-122.
- Waters, A. C. (1961), Basalt magma types and their tectonic associations: Pacific Northwest of the United States, in The crust of the Pacific basin. Am. Geop. Union Monograph No. 6, p. 158-170.
- Wilcox, R. E. (1954), Petrology of the Paricutin volcano, Mexico. U.S.G.S. Bull. 965-C, p. 281-344.
- Williams, H., F. J. Turner, and C. M. Gilbert (1955), Petrography W. H. Freeman Co., San Francisco, 406 p.
- Yoder, H. S. and C. E. Tilley (1962), The origin of basalt magmas: An experimental study of natural and synthetic rock systems. Jour. Pet., Vol. 3, p. 342-532.

/